© 2019. Published by The Company of Biologists Ltd | Development (2019) 146, dev171009. doi:10.1242/dev.171009

STEM CELLS AND REGENERATION

RESEARCH ARTICLE

Multiple supporting cell subtypes are capable of spontaneous hair cell regeneration in the neonatal mouse cochlea

Melissa M. McGovern[1], Michelle R. Randle[1], Candice L. Cuppini[1], Kaley A. Graves[1] and Brandon C. Cox[1,2,*]

ABSTRACT

Supporting cells (SCs) are known to spontaneously regenerate hair cells (HCs) in the neonatal mouse cochlea, yet little is known about the relative contribution of distinct SC subtypes which differ in morphology and function. We have previously shown that HC regeneration is linked to Notch signaling, and some SC subtypes, but not others, lose expression of the Notch effector *Hes5*. Other work has demonstrated that Lgr5-positive SCs have an increased capacity to regenerate HCs; however, several SC subtypes express Lgr5. To further investigate the source for spontaneous HC regeneration, we used three CreER lines to fate-map distinct groups of SCs during regeneration. Fate-mapping either alone or combined with a mitotic tracer showed that pillar and Deiters' cells contributed more regenerated HCs overall. However, when normalized to the total fate-mapped population, pillar, Deiters', inner phalangeal and border cells had equal capacity to regenerate HCs, and all SC subtypes could divide after HC damage. Investigating the mechanisms that allow individual SC subtypes to regenerate HCs and the postnatal changes that occur in each group during maturation could lead to therapies for hearing loss.

KEY WORDS: Supporting cell subtypes, Mitotic regeneration, Fate-mapping, Pillar cells, Deiters' cells, Inner phalangeal cells

INTRODUCTION

The spiral shaped cochlea that is located within the inner ear contains specialized sensory cells, called hair cells (HCs), which are necessary for hearing. Sound waves traveling through the fluid-filled cochlea deflect the stereocilia bundles that are located on the apical surface of HCs, which causes depolarization. This activates afferent spiral ganglion neurons, thus relaying information to central auditory structures. HCs are surrounded by supporting cells (SCs) which have numerous functions such as releasing trophic factors, taking-up ions and neurotransmitters, and phagocytosing dying HCs (Abrashkin et al., 2006; Anttonen et al., 2014; Flores-Otero et al., 2007; Furness et al., 2002; Gómez-Casati et al., 2010a; Kikuchi et al., 2000; Sugawara et al., 2007; Zuccotti et al., 2012).

During embryonic development of the mammalian cochlea, HCs and SCs develop from the same pool of progenitor cells (reviewed by Basch et al., 2016). When HCs are killed by ototoxic medications, noise or the consequences of aging, hearing is impaired because the mature mammalian cochlea cannot regenerate auditory HCs (Bohne, 1976; Hawkins et al., 1976; Maass et al., 2015; Oesterle et al., 2008). In contrast, the sensory organs of birds, fish and amphibians can spontaneously regenerate HCs throughout their lifespan (Balak et al., 1990; Corwin and Cotanche, 1988; Jones and Corwin, 1996; Ryals and Rubel, 1988; Shang et al., 2010; Stone and Cotanche, 2007; Warchol and Corwin, 1996). This occurs by both mitotic regeneration, in which SCs divide before taking an HC fate, and direct transdifferentiation, in which SCs directly change cell fate and convert into HCs in the absence of cell division (reviewed by Rubel et al., 2013).

Recently, evidence has emerged that the neonatal mouse cochlea has a limited period in which it is capable of spontaneously regenerating HCs after they have been destroyed, both *in vivo* (Cox et al., 2014; Hu et al., 2016; McGovern et al., 2018) and *in vitro* (Bramhall et al., 2014). To demonstrate that regeneration had occurred, broad populations of SCs were fate-mapped using either $Hes5^{lacZ}$ knock-in reporter mice, $Lgr5^{CreER}$::$Rosa26^{tdTomato}$ mice or $Sox2^{CreERT2}$::$Rosa26^{tdTomato}$ mice (Bramhall et al., 2014; Cox et al., 2014). Co-expression of β-galactosidase or tdTomato with HC markers after damage provided evidence that regenerated HCs were derived from the SC population. In addition, a small percentage of newly generated, fate-mapped HCs also incorporated a mitotic tracer, which indicated that some SCs divided before converting into an HC. Although this evidence indicates that SCs are the source of regenerated HCs, potential differences in the regenerative plasticity of SC subtypes is still unclear. Some have hypothesized that Lgr5-positive SCs are the progenitor cells within the neonatal mouse cochlea (Bramhall et al., 2014; Chai et al., 2012; McLean et al., 2017; Shi et al., 2012; Shi et al., 2013; Waqas et al., 2016); however, the Lgr5-postive population includes different subtypes of SCs, and the expression of Lgr5 changes dynamically during the first postnatal week (Chai et al., 2011; Shi et al., 2012). In addition, we have recently shown that spontaneous HC regeneration *in vivo* can be prevented by increased Notch signaling (McGovern et al., 2018), which suggests that the SC subtypes that respond to changes in Notch signaling after HC damage contribute to spontaneous regeneration.

SCs can be separated into at least eight distinct subtypes: cells of the greater epithelial ridge (GER), inner phalangeal cells (IPhCs), border cells (BCs), inner pillar cells (PCs), outer PCs, Deiters' cells (DCs), Hensen cells (HeCs) and Claudius cells (CCs) (Jahan et al., 2015; Raphael and Altschuler, 2003). Previous studies have shown differences in the plasticity of these subtypes. For example, neonatal and juvenile PCs, DCs and IPhCs/BCs are able to convert into HCs after ectopic *Atoh1* expression (Liu et al., 2012a; Liu et al., 2014; Walters et al., 2017). Furthermore, PCs and DCs proliferate after the cell cycle regulator retinoblastoma is deleted (Yu et al., 2010). Yet when the cell cycle inhibitor $p27^{Kip1}$ (also known as *Cdkn1b*) or the transcription factor *Sox2* is deleted, only inner PCs proliferate (Liu et al., 2012b). Moreover, when IPhCs and BCs are ablated at birth, cells of the GER are capable of regenerating them and hearing in the

[1]Department of Pharmacology, Southern Illinois University School of Medicine, Springfield, IL 62711, USA. [2]Department of Surgery, Division of Otolaryngology, Southern Illinois University School of Medicine, Springfield, IL 62711, USA.

*Author for correspondence (bcox@siumed.edu)

B.C.C., 0000-0002-6989-161X

Received 14 August 2018; Accepted 9 January 2019

Development (2019) 146, dev171009. doi:10.1242/dev.171009

mature cochlea of these mice is normal (Mellado Lagarde et al., 2014). In contrast, when PCs and DCs are ablated at birth they are not replaced by neighboring cells, therefore subsequent HC death and hearing loss occurs (Mellado Lagarde et al., 2013).

We recently showed that, during the spontaneous HC regeneration process, PCs and DCs lose expression of *Hes5*, a Notch effector and inhibitor of HC fate (Abdolazimi et al., 2016; Mulvaney and Dabdoub, 2012), whereas IPhCs and BCs showed no change in *Hes5* expression (McGovern et al., 2018). This may suggest that PCs and DCs have an increased ability to regenerate HCs compared with other SC subtypes, yet further investigation is needed. To address this question in the present study, we fate-mapped three different groups of SCs using CreER/loxP mouse models after HC ablation in the neonatal mouse cochlea. We also investigated changes in the expression of $p27^{Kip1}$ after HC damage, as well as used fate-mapping in combination with a mitotic tracer to determine which SC subtypes could divide before converting into HCs. Although the majority of spontaneously regenerated HCs detected either with or without a mitotic tracer were derived from PCs and DCs, when the data was normalized to the total pool of tdTomato-labeled SCs in control samples of each CreER line, PCs, DCs, IPhCs and BCs were equally capable of regenerating HCs. However, there was no evidence that the regenerated HCs were derived from HeCs or cells in the GER. Further investigation of the maturation process that occurs in these SC subtypes during the perinatal period will inform future investigations aimed at stimulating HC regeneration in the mature cochlea.

RESULTS

IPhCs, BCs, PCs and DCs contribute to spontaneous HC regeneration

To determine which SC subtypes within the neonatal cochlea spontaneously regenerate HCs after damage, we used three different CreER lines paired with the $Rosa26^{CAG\text{-}loxP\text{-}stop\text{-}loxP\text{-}tdTomato}$ ($Rosa26^{tdTomato}$) reporter to fate-map three groups of SC subtypes. $Prox1^{CreERT2}::Rosa26^{tdTomato}$, $Plp\text{-}CreER^{T2}::Rosa26^{tdTomato}$ and $GLAST\text{-}CreER^{T2}::Rosa26^{tdTomato}$ mice were bred with $Pou4f3^{DTR}$ mice, which express the human diphtheria toxin receptor (DTR) in HCs, and injection of diphtheria toxin (DT) results in HC ablation (Golub et al., 2012; Tong et al., 2015). All mice were injected with tamoxifen [3 mg/40 g, intraperitoneally (IP)] at postnatal day (P) 0 to induce tdTomato expression in SCs, followed by DT injection [6.25 ng/g, intramuscularly (IM)] at P1 to induce HC damage and thus spontaneous HC regeneration. Cochleae were collected at P7 and analyzed using confocal microscopy to visualize endogenous tdTomato fluorescence, and co-labeled with antibodies against myosin VIIa (to label HCs) and Sox2 (to label all SC and immature HC nuclei). The entire organ of Corti was imaged, measured and divided into six equal segments, starting in the apex as previously described (McGovern et al., 2017). The total number of cells that expressed both tdTomato and myosin VIIa throughout the entire cochlea was quantified to determine how many regenerated HCs originated from each group of fate-mapped SC subtypes. Of note, we have previously shown that the number of Sox2-positive cells is reduced during the window of regeneration as SCs convert into HCs (McGovern et al., 2018). Similarly, we observed a qualitative reduction in Sox2-positive cells in all three CreER lines. It is unlikely that SCs die after HC ablation, as DT-mediated cell death is known to occur in a cell autonomous fashion (Abrahamsen et al., 2008; Ivanova et al., 2005) and DT-mediated HC death did not affect SC survival when DT was injected at an older age when HC regeneration does not occur (Tong et al., 2015).

$Prox1^{CreERT2}::Rosa26^{tdTomato}$ mice that were injected with tamoxifen at P0 label the majority of PCs and DCs, but no other cell type and no cells were labeled without tamoxifen administration (McGovern et al., 2017). In $Prox1^{CreERT2}::Rosa26^{tdTomato}$ control samples, which lacked $Pou4f3^{DTR}$ and therefore lacked HC damage, 7.7±1.8 tdTomato/myosin VIIa double positive cells were detected in the most apical tip of the cochlea (n=4; data are mean±s.e.m.; Fig. 1A-B″,D). However, significantly more tdTomato/myosin VIIa double positive cells were found throughout the cochlea of $Prox1^{CreERT2}::Rosa26^{tdTomato}::Pou4f3^{DTR}$ mice (50.8±7.6; P<0.01; Student's t-test; n=4; Fig. 1C-D). The majority of these tdTomato-positive HCs were detected in the first apical segment, and the number declined in an apical to basal gradient (35.7±7.6 in the most apical segment versus 0.0±0.0 in the most basal segment; r^2=0.5514; P=0.0001; n=4; Fig. 1D).

$Plp\text{-}CreER^{T2}::Rosa26^{tdTomato}$ mice that were injected with tamoxifen at P0 predominantly label IPhCs and BCs, but no cells were labeled without tamoxifen administration (McGovern et al., 2017). $Plp\text{-}CreER^{T2}::Rosa26^{tdTomato}$ cochleae, which lacked $Pou4f3^{DTR}$ and therefore HC damage, had a small number (2.0±0.9) of tdTomato/myosin VIIa double positive cells in the apical tip of the cochlea (n=4; Fig. 2A-B″,D). After HC damage however, significantly more tdTomato/myosin VIIa double positive cells were detected in $Plp\text{-}CreER^{T2}::Rosa26^{tdTomato}::Pou4f3^{DTR}$ mice (20.2 ±5.5; P<0.05; Student's t-test; n=4; Fig. 2C-D). Again, there was an apical to basal gradient of regenerated HCs with 14.2±2.6 HCs in the apical third of the cochlea compared with 1.0±0.7 in the basal third (n=4; r^2=0.3912; P=0.0011; Fig. 2D).

A single tdTomato-positive HC was detected at P7 in one of the control $GLAST\text{-}CreER^{T2}::Rosa26^{tdTomato}$ samples that did not receive tamoxifen (Fig. 3A-D). $GLAST\text{-}CreER^{T2}::Rosa26^{tdTomato}$ mice that were injected with tamoxifen at P0 label 46.9%±15.2% of the cells in the GER, 48.8%±6.2% IPhCs/BCs, as well as 24.3% ±18.8% HeCs, whereas less than 3% of PCs and DCs were labeled (Fig. 3E-H,I). $GLAST\text{-}CreER^{T2}::Rosa26^{tdTomato}$ cochleae that lacked the $Pou4f3^{DTR}$ allele, had 4.0±1.0 tdTomato/myosin VIIa double positive cells in the most apical tip (n=4; Fig. 4A-B″,D). In $GLAST\text{-}CreER^{T2}::Rosa26^{tdTomato}::Pou4f3^{DTR}$ mice, the number of tdTomato/myosin VIIa double positive cells after HC damage and spontaneous HC regeneration was not significantly different from the control (13.5±4.0; P=0.6; Student's t-test; n=4; Fig. 4C-D) which indicates that cells fate-mapped by $GLAST\text{-}CreER^{T2}$ (cells of the GER, IPhCs, BCs, and HeCs) do not contribute to spontaneous HC regeneration.

The majority of spontaneously regenerated HCs are produced by PCs and DCs

To compare the number of regenerated HCs between CreER lines, we first assessed whether the level of HC damage and regeneration was equivalent across lines. Unfortunately, tools to accurately quantify the total number of regenerated HCs are currently unavailable as myosin VIIa labeling alone represents a mix of surviving HCs, regenerated HCs and HC corpses that have not been cleared from the sensory epithelium (S. Francis and L. Cunningham, unpublished). Therefore, we assessed HC damage and regeneration indirectly in two ways: by normalizing numbers of myosin VIIa-positive cells left after HC loss to undamaged controls and by comparing the number of Sox2-positive immature HCs after regeneration was induced. Previous studies have shown that newly differentiated HCs express Sox2 until P0-P1 (Dabdoub et al., 2008; Hume et al., 2007; Kempfle et al., 2016; Kiernan et al., 2005; Mak et al., 2009). In addition, during spontaneous regeneration, Sox2-expressing SCs convert into HCs,

Development (2019) 146, dev171009. doi:10.1242/dev.171009

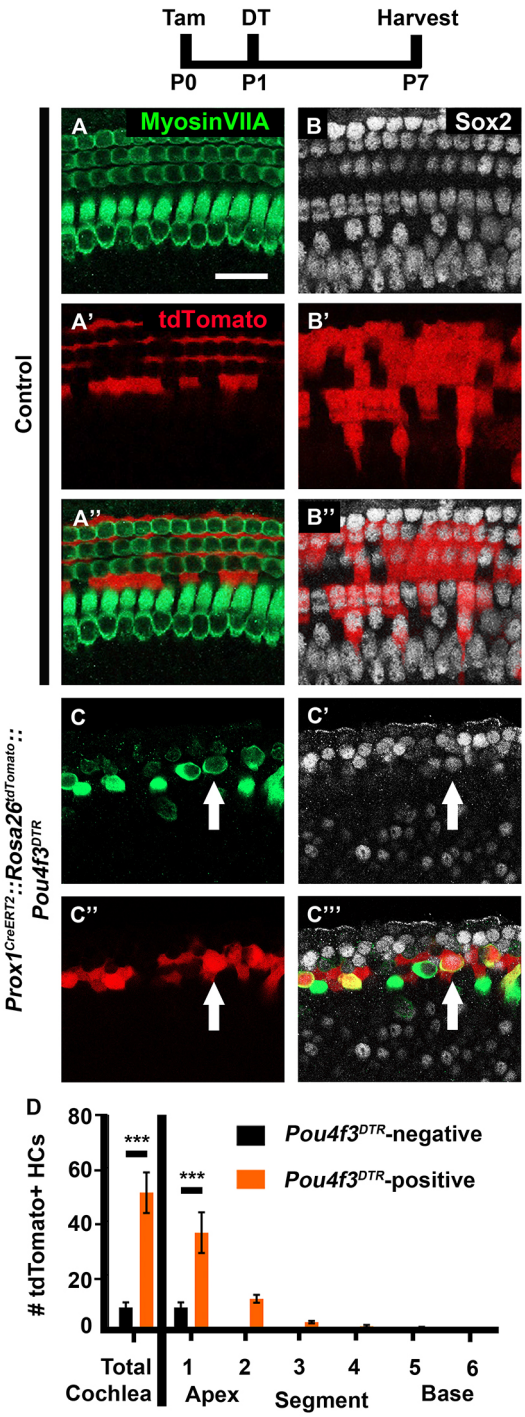

Fig. 1. PCs and DCs spontaneously regenerate HCs in the neonatal mouse cochlea. (A-C‴) Representative confocal slice images from P7 *Prox1*^{CreERT2}*::Rosa26*^{tdTomato}*::Pou4f3*^{DTR} mice (C-C‴) as well as littermate controls that lacked *Pou4f3*^{DTR} (A-B″). All mice were injected with tamoxifen (Tam) at P0 to induce tdTomato expression among PCs/DCs, and with diphtheria toxin (DT) at P1 to induce HC death in the experimental samples. Anti-myosin VIIa antibodies were used to label HCs (green); anti-Sox2 antibodies were used to label SC and immature HC nuclei (white); tdTomato was detected using endogenous fluorescence (red). Arrows indicate tdTomato-positive, regenerated HCs. Scale bar: 50 µm. (D) Quantification of fate-mapped HCs in the six segments of the cochlea show that PCs/DCs spontaneously regenerate HCs and that the majority of tdTomato-positive HCs are present in the first apical segment of the cochlea. ***P<0.001, determined using either a Student's t-test (for total cochlea) or a two-way ANOVA with a Sidak's post-hoc test (for the six segments). Data are mean±s.e.m.; n=4.

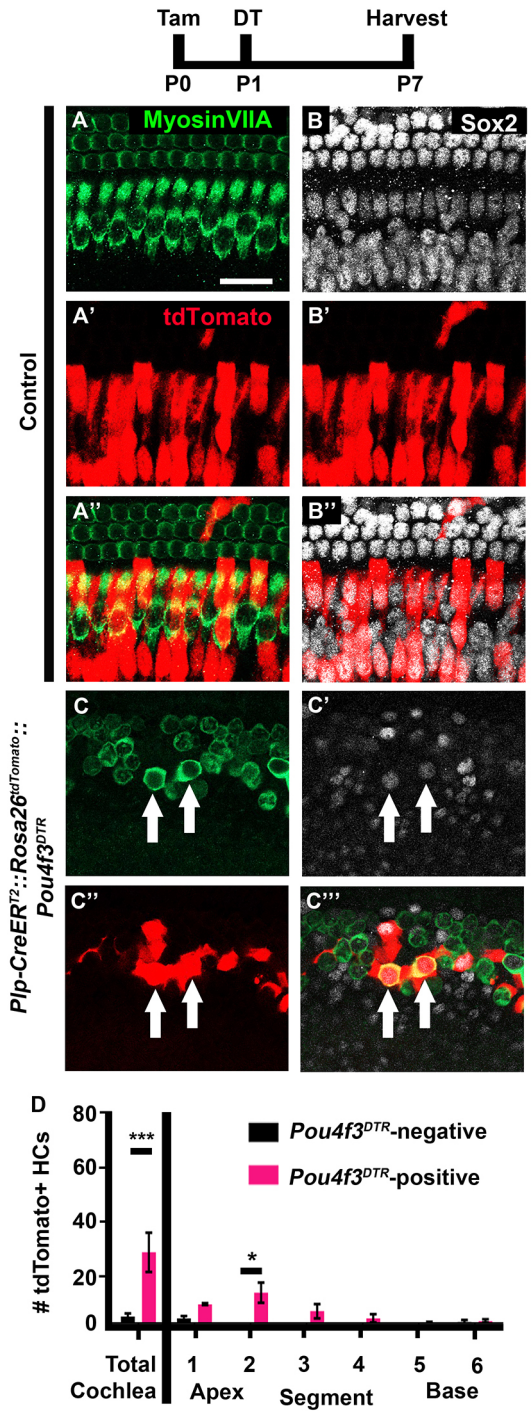

Fig. 2. IPhCs and BCs spontaneously regenerate HCs in the neonatal mouse cochlea. (A-C‴) Representative confocal slice images from P7 *Plp-CreER*^{T2}*::Rosa26*^{tdTomato}*::Pou4f3*^{DTR} mice (C-C‴), as well as littermate controls that lacked *Pou4f3*^{DTR} (A-B″). All mice were injected with tamoxifen (Tam) at P0 to induce tdTomato expression in IPhCs/BCs and with diphtheria toxin (DT) at P1 to induce HC death in the experimental samples. Anti-myosin VIIa antibodies were used to label HCs (green); anti-Sox2 antibodies were used to label SC and immature HC nuclei (white); tdTomato was detected using endogenous fluorescence (red). Arrows indicate tdTomato-positive, regenerated HCs. Scale bar: 50 µm. (D) Quantification of fate-mapped HCs in the six segments of the cochlea show that more tdTomato-positive HCs were detected after HC damage compared with *Pou4f3*^{DTR}-negative controls. ***P<0.001, determined using a Student's t-test (for total cochlea); *P<0.05, determined using a two-way ANOVA with a Sidak's post-hoc test (for the six segments). Data are mean±s.e.m.; n=4.

Development (2019) 146, dev171009. doi:10.1242/dev.171009

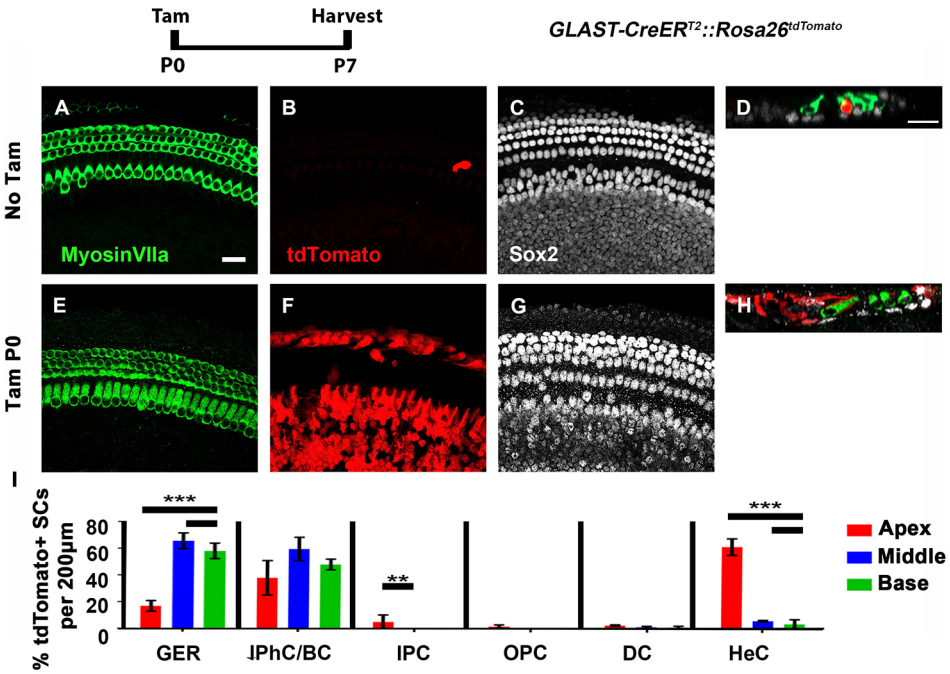

Fig. 3. *GLAST-CreER^{T2}* is expressed in cells of the GER, IPhCs/BCs and HeCs in the neonatal cochlea. (A-H) Representative confocal maximum projection images from P7 *GLAST-CreER^{T2}::Rosa26^{tdTomato}* controls that were not injected with tamoxifen (Tam) (A-D) or experimental mice that were injected with Tam at P0 to induce tdTomato expression (E-H). Anti-Sox2 antibodies were used to detect Sox2 expression in the nuclei of SCs (white), and anti-myosin VIIa antibodies were used to label HCs (green). tdTomato was detected through endogenous fluorescence (red). D and H show optical cross-sections of the image shown in A-C and E-G, respectively. (I) The percentage of tdTomato/Sox2-double positive cells was quantified for each SC subtype. *GLAST-CreER^{T2}::Rosa26^{tdTomato}* predominantly labels cells of the GER and IPhCs/BCs, as well as HeCs. ***P<0.001, **P<0.01, determined using a two-way ANOVA. Data are mean±s.e.m.; n=3. Scale bars: 20 µm.

after which Sox2 expression is downregulated after several days (Cox et al., 2014). We first quantified the number of myosin VIIa-positive HCs in two 200 µm regions per cochlear turn in undamaged controls, as well as in samples with HC damage and regeneration. Myosin VIIa cells were expressed as a percentage of remaining HCs, including regenerated HCs, HC corpses and those that survived damage. If all groups had the same level of HC damage and regeneration, the number of remaining HCs across samples should remain consistent among CreER lines. As expected, the number of myosin VIIa-positive cells after DT-induced HC damage and spontaneous HC regeneration was not significantly different across the three mouse lines (67.9%±3.9% in *Prox1^{CreERT2}*, 69.6%±5.2% in *Plp-CreER^{T2}* and 66.9%±8.2% in *GLAST-CreER^{T2}*; n=3; Fig. 5A). There was also no difference in the number of Sox2-positive regenerated HCs among CreER lines (28.0±8.9 in *Prox1^{CreERT2}*, 28.3±2.3 in *Plp-CreER^{T2}* and 32.3±11.3 in *GLAST-CreER^{T2}*; n=3; Fig. 5B). Therefore, we concluded that the level of HC regeneration was consistent between CreER lines.

To understand which SC subtypes contribute regenerated HCs, we investigated the number of tdTomato-positive SCs of each subtype in control cochlea. Similar to previous reports, *Prox1^{CreERT2}* labeled only PCs and DCs, yet fewer inner PCs were labeled than outer PCs (30.0%±5.0% IPCs, 81.3±9.3% OPCs and 85.1%±2.5% DCs, P<0.001; n=3; Fig. 5C,D; McGovern et al., 2017; Mellado Lagarde et al., 2014; Yu et al., 2010). *Plp-CreER^{T2}* labeled 51.8%±12.3% IPhCs/BCs and ∼6-12% of PCs and DCs, which is similar to previous studies (n=3, Fig. 5C,D; Cox et al., 2012; Doerflinger et al., 2003; Gómez-Casati et al., 2010b; McGovern et al., 2017; Mellado Lagarde et al., 2014). *GLAST-CreER^{T2}* labeled 38.2%±12.9% IPhCs/BCs, 17.0%±4.0% cells of the GER, 62.0%±6.1% HeCs and ∼2-5% of PCs/DCs (Fig. 5C-D; Mellado Lagarde et al., 2014). Therefore, *Prox1^{CreERT2}* labeled more outer PCs (∼81%) and DCs (∼85%) than either *Plp-CreER^{T2}* (∼10% outer PCs and ∼6% DCs; P<0.001) or *GLAST-CreER^{T2}* (∼2% outer PCs and ∼3% DCs; P<0.001). *Prox1^{CreERT2}* also labeled more inner PCs (∼30%) than *GLAST-CreER^{T2}* (∼5%; P<0.05), but there was no difference from *Plp-CreER^{T2}* (∼12%). Both *Plp-CreER^{T2}* and *GLAST-CreER^{T2}* labeled more IPhCs/BCs (∼52% for *Plp-CreER^{T2}* and ∼38% for *GLAST-CreER^{T2}*) than *Prox1^{CreERT2}* (0%; P<0.001 and P<0.01, respectively), although they were not different from each other. Finally, *GLAST-CreER^{T2}* labeled more HeCs (∼62%) than either *Prox1^{CreERT2}* or *Plp-CreER^{T2}* (both 0%; P<0.001).

We then compared the total number of fate-mapped, regenerated HCs from each lineage that was significantly different from control samples to determine the relative contribution of the SC subtypes that were fate-mapped by each CreER line. Significantly more tdTomato/myosin VIIa-double positive cells (regenerated HCs) were derived from PCs and DCs labeled by *Prox1^{CreERT2}* (50.7±7.5; n=4) than IPhCs and BCs labeled by *Plp-CreER^{T2}* (20.2±5.5; P=0.05; n=4; Fig. 5E). Therefore, PCs and DCs contribute more regenerated HCs than other SC subtypes within the neonatal cochlea.

PCs, DCs, and IPhCs/BCs have a similar capacity for spontaneous HC regeneration

We next investigated whether the increased number of regenerated HCs that were produced by PCs and DCs are the result of their increased capacity to convert into HCs, or whether PCs and DCs collectively constitute a larger pool of SCs that were fate-mapped. To investigate the capacity of each pool of SCs to spontaneously regenerate HCs, we normalized the number of fate-mapped regenerated HCs to the number of tdTomato-labeled SCs in controls without HC damage for each CreER line. *Prox1^{CreERT2}::Rosa26^{tdTomato}* cochleae had a larger number of tdTomato-positive SCs (2375±26.9) than *Plp-CreER^{T2}* (1232±241.3; P=0.003; n=3; Fig. 5F). However the SC-to-HC conversion rate of *Prox1^{CreERT2}::Rosa26^{tdTomato}* mice (2.1%±0.6%) was not significantly different than the rate of conversion in *Plp-CreER^{T2}::Rosa26^{tdTomato}* cochleae (1.6%±0.9%; Fig. 5G). This indicates that IPhCs, BCs, PCs, and DCs have the same capacity to convert into HCs after HC loss at birth.

Loss of the cell cycle inhibitor *p27^{Kip1}* was limited to PCs and DCs

Previous studies have shown that spontaneous HC regeneration in the neonatal mouse cochlea occurs by two cellular mechanisms:

Development (2019) 146, dev171009. doi:10.1242/dev.171009

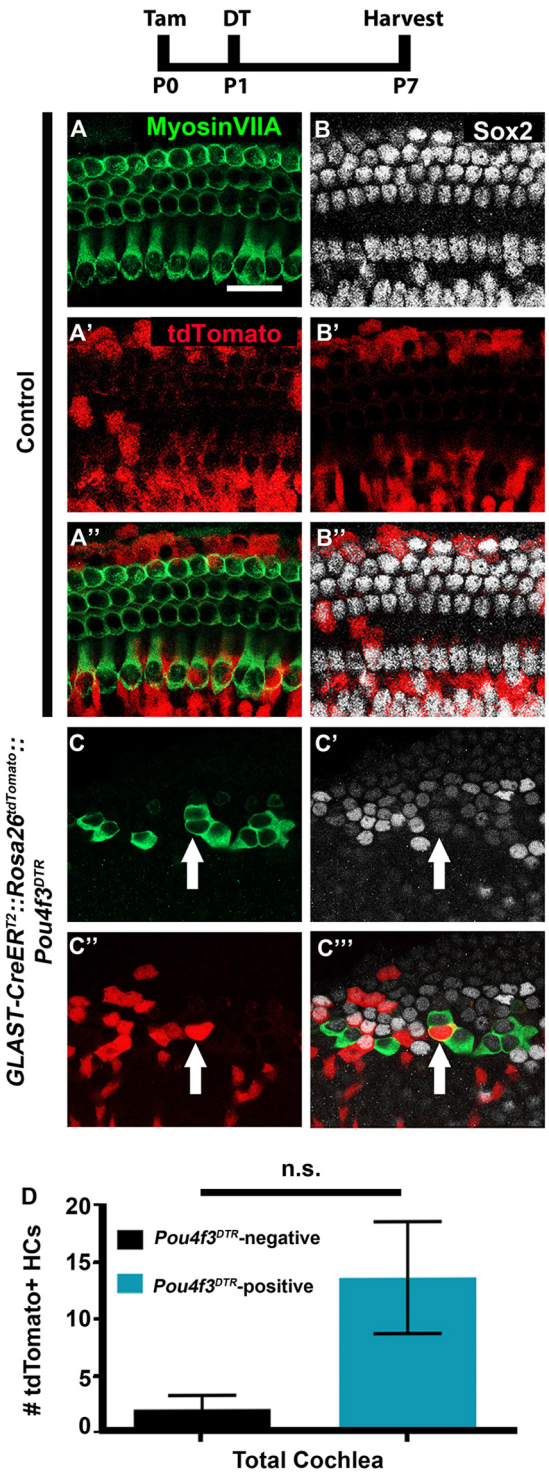

Fig. 4. Cells of the GER and HeCs do not regenerate HCs after HC damage. (A-C‴) Representative confocal slice images from P7 *GLAST-CreER^{T2}::Rosa26^{tdTomato}::Pou4f3^{DTR}* mice (C-C‴) as well as littermate controls that lacked *Pou4f3^{DTR}* (A-B‴). All mice were injected with tamoxifen (Tam) at P0 to induce tdTomato expression in cells of the GER, IPhCs/BCs and HeCs, and with diphtheria toxin (DT) at P1 to induce HC death in the experimental samples. Anti-myosin VIIa antibodies were used to label HCs (green); anti-Sox2 antibodies were used to label SC and immature HC nuclei (white); tdTomato was detected using endogenous fluorescence (red). Arrows indicate tdTomato-positive HCs. Scale bar: 50 µm. (D) Quantification shows no increase in the number of tdTomato-positive HCs after HC damage compared with *Pou4f3^{DTR}*-negative controls, determined using a Student's *t*-test. Data are mean±s.e.m.; *n*=4. n.s., not significant.

direct transdifferentiation, in which SCs directly change cell fate and convert into HCs, and mitotic regeneration, in which SCs first divide and one or both daughter cells take an HC fate (Cox et al., 2014; Hu et al., 2016). One study fate-mapped Lgr5-positive cells along with a mitotic tracer and observed a small number of mitotically regenerated HCs from both fate-mapped and non-fate-mapped lineages (Cox et al., 2014). Therefore, some Lgr5-positive SCs are capable of mitotic HC regeneration, and there are also other unknown SC subtypes that are capable of this function. SC subtypes capable of mitotically regenerating HCs are of interest because they can replenish both the HC and SC population.

To investigate which SC subtypes are capable of mitotic HC regeneration, we investigated changes in the expression of the cell cycle inhibitor *p27^{Kip1}* after HC damage and during the window of spontaneous HC regeneration. *p27^{Kip1}* is a cyclin-dependent kinase inhibitor which inhibits cyclin D during the G1 phase of the cell cycle (Toyoshima and Hunter, 1994). During embryonic cochlear development, *p27^{Kip1}* is upregulated in all progenitor cells as they exit the cell cycle between embryonic day (E) 12.5-14.5 and its expression is maintained in all SCs throughout the life of the animal (Chen and Segil, 1999; Lee et al., 2006; Oesterle et al., 2011). Interestingly, SCs that are isolated from the neonatal mouse organ of Corti and grown in culture are capable of downregulating *p27^{Kip1}*, incorporating the mitotic tracer 5-bromo-2-deoxyuridine (BrdU) and differentiating into HC-like cells (White et al., 2006). This suggests that SCs that downregulate *p27^{Kip1}* in the cochlea are likely capable of undergoing cell division.

Atoh1-CreER^{TM}::Rosa26$^{loxP\text{-}stop\text{-}loxP\text{-}DTA}$ mice (hereafter referred to as *Atoh1-DTA*) were previously used to induce HC damage and regeneration in the neonatal mouse cochlea (Cox et al., 2014; McGovern et al., 2018). *Atoh1-DTA* mice and littermate controls, which lack either the *Atoh1-CreER^{TM}* or *Rosa26^{DTA}* allele, were injected with tamoxifen (3 mg/40 g, IP) on P0 and P1 to induce HC damage and thus spontaneous HC regeneration. S100a1 is a calcium binding protein that was previously used to segregate the PC/DC population from IPhCs/BCs after the tissue was disorganized by HC loss and regeneration (McGovern et al., 2018). Here, we used S100a1 to label PCs/DCs in order to determine whether any groups of SCs lose *p27^{Kip1}* expression after HC loss. Using the apical turn at P2 and P4, we quantified the number of cells that expressed Sox2 but lacked p27^{Kip1} in both S100a1-positive and S100a1-negative SCs. In undamaged control cochleae, all SCs expressed p27^{Kip1} (Fig. 6A-A‴). After HC damage was induced at birth, 7.0±1.0 Sox2-positive/S100a1-positive/p27^{Kip1}-negative cells were detected at P2 (P<0.001 compared with P2 controls 0±0; n=4) and 2.6±1.6 cells were detected at P4 (not significant compared with controls 0±0; n=4; Fig. 6B-E). All Sox2-positive/p27^{Kip1}-negative cells observed were also S100a1-positive, which indicates that they were PCs and DCs. This indicates that, during the window of spontaneous HC regeneration, some PCs and DCs lose the cell cycle inhibitor *p27^{Kip1}*, which suggests that they may be the population of SCs that are capable of mitotic HC regeneration.

A larger proportion of mitotically regenerated HCs were derived from PCs and DCs

Loss of *p27^{Kip1}* is only suggestive that a cell is entering the cell cycle. Therefore we combined a mitotic tracer with fate-mapping, using the same CreER mouse lines from above, to investigate the ability of the three groups of SCs to mitotically regenerate cochlear HCs, as well as repopulate the SC population. As before, *Prox1^{CreERT2}::Rosa26^{tdTomato}::Pou4f3^{DTR}* mice, *PlpCre^{ERT2}::Rosa26^{tdTomato}::Pou4f3^{DTR}* mice and *GLAST-CreER^{T2}::Rosa26^{tdTomato}::*

Development (2019) 146, dev171009. doi:10.1242/dev.171009

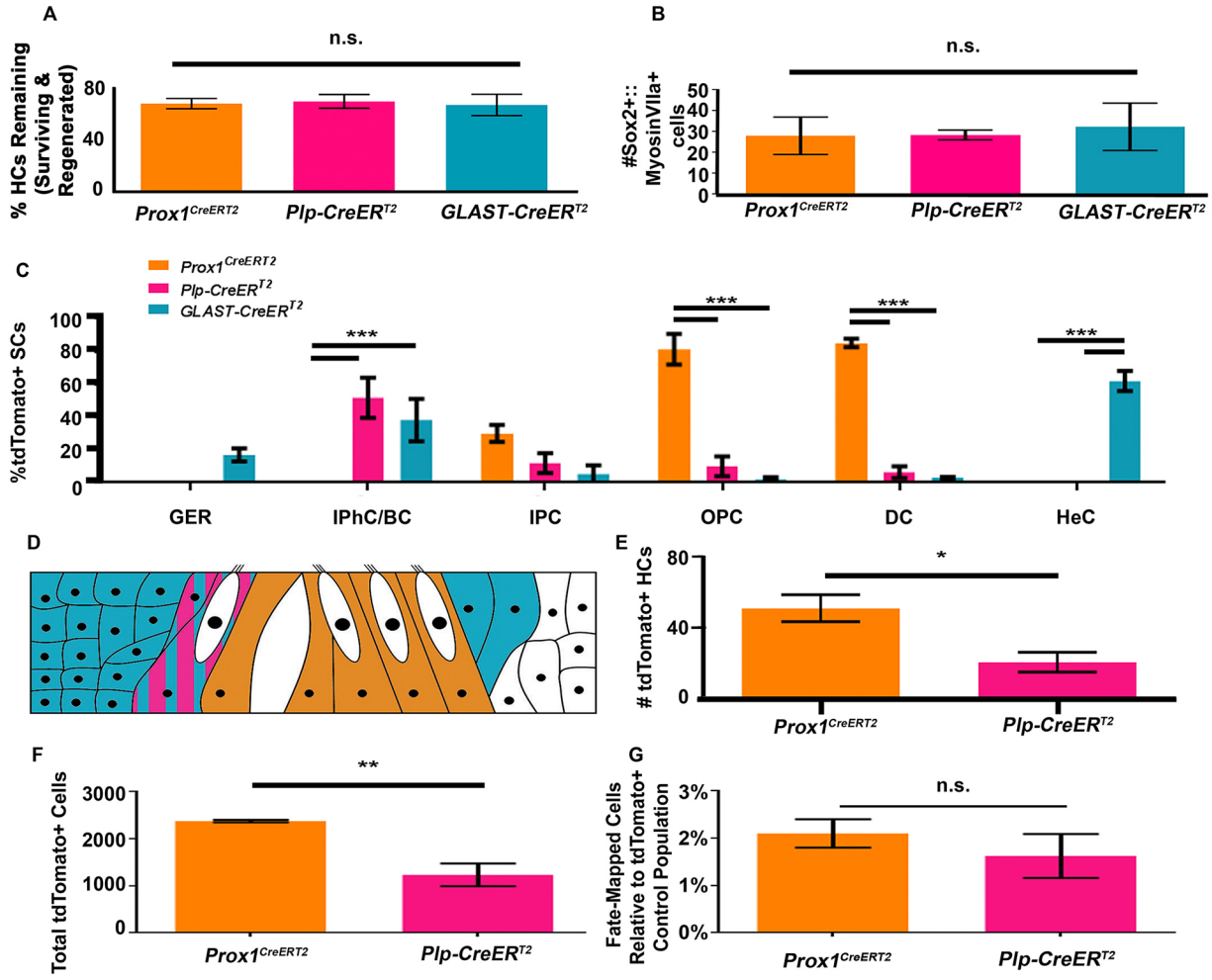

Fig. 5. All three CreER lines had consistent amounts of HC damage and the majority of spontaneously regenerated HCs are derived from PCs and DCs. (A) There was no significant difference in the percentage of remaining HCs (surviving plus regenerated HCs) among the three CreER lines, determined using a one-way ANOVA. (B) There was no significant difference in the number of Sox2-positive/myosin VIIa-positive cells after HC loss and regeneration were induced, determined using a one-way ANOVA. This indicates that the level of regeneration among each CreER line was similar. (C) *Prox1*^{CreERT2} specifically labels inner PCs, outer PCs and DCs; *Plp-CreER*^{T2} predominantly labels IPhCs/BCs, with few inner PCs, outer PCs and DCs labeled; *GLAST-CreER*^{T2} labels predominantly cells of the GER, IPhCs/BCs and HeCs, with few PCs and DCs labeled. ***P<0.001, determined using a two-way ANOVA with a Tukey's post-hoc test. (D) Schematic of the expression patterns for CreER lines used for fate mapping. *Glast-CreER*^{T2} (teal) is expressed in cells of the GER, IPhCs/BCs and HeCs. *Prox1*^{CreERT2} (orange) is expressed in PCs and DCs. *Plp-CreER*^{T2} (magenta) is expressed in IPhCs/BCs. (E) Significantly more tdTomato-positive, regenerated HCs were observed when *Prox1*^{CreERT2} was used for fate-mapping compared with *Plp-CreER*^{T2}. *P<0.05, determined using a Student's *t*-test. (F) More SCs were labeled by tdTomato in *Prox1*^{CreERT2} cochleae compared with *Plp-CreER*^{T2} cochleae. **P<0.01, determined using Student's *t*-test. (G) The total number of fate-mapped regenerated HCs was normalized to the total number of tdTomato-labeled SCs in control samples of each CreER line. Both CreER lines had an equal capacity to regenerate HCs, determined using a Student's *t*-test. Data are mean±s.e.m. n.s., not significant.

Pou4f3^{DTR} mice, as well as controls that lacked the *Pou4f3*^{DTR} allele, were injected with tamoxifen (3 mg/40 g, IP) at P0 to induce *tdTomato* expression among the specific SC populations, followed by DT injection (6.25 ng/g, IM) at P1 to induce HC damage in *Pou4f3*^{DTR}-positive mice. To label mitotically active cells, mice were also injected with BrdU (50 mg/kg, IP) twice per day from P3-P6 with ∼6 h between injections. Cochleae were collected at P6-P7 (due to unexpected high mortality rates, some samples were collected on P6 at least 30 min after the last BrdU injection). For each of the three mouse models, we quantified the total number of mitotically regenerated HCs in the cochlea that were fate-mapped (BrdU-positive/tdTomato-positive/myosin VIIa-positive cells), mitotically regenerated HCs that were not fate-mapped (BrdU-positive/tdTomato-negative/myosin VIIa-positive cells) and fate-mapped mitotically active SCs that remained as SCs (BrdU-positive/tdTomato-positive/myosin VIIa-negative cells).

In control samples, no BrdU-positive/myosin VIIa-positive cells were seen in any samples (Fig. 7A,C,E). The only BrdU-positive/tdTomato-positive/myosin VIIA-negative cells (mitotically active SCs that remained as SCs) observed in control samples were located in the cells of the GER from *GLAST-CreER*^{T2}*::Rosa26*^{tdTomato} mice (data not shown), which is consistent with previous reports (Oesterle et al., 2011; Taniguchi et al., 2012). In experimental samples, there was no significant difference in the total number of fate-mapped, mitotically active SCs that remained as SCs (BrdU-positive/tdTomato-positive/myosin VIIa-negative cells) among CreER lines (28.0±11.2 for *Prox1*^{CreERT2}, 18.4±4.7 for *Plp-CreER*^{T2} and 20.3 ±9.8 for *GLAST-CreER*^{T2}; n=3; Fig. 7G). Although there was also no significant difference in the total number of fate-mapped, mitotically regenerated HCs (BrdU-positive/tdTomato-positive/myosin VIIa-positive cells) among the three lineages (2.6±0.33 in *Prox1*^{CreERT2}, 1.3±0.8 in *Plp-CreER*^{T2} and 0.3±0.3 in

Development (2019) 146, dev171009. doi:10.1242/dev.171009

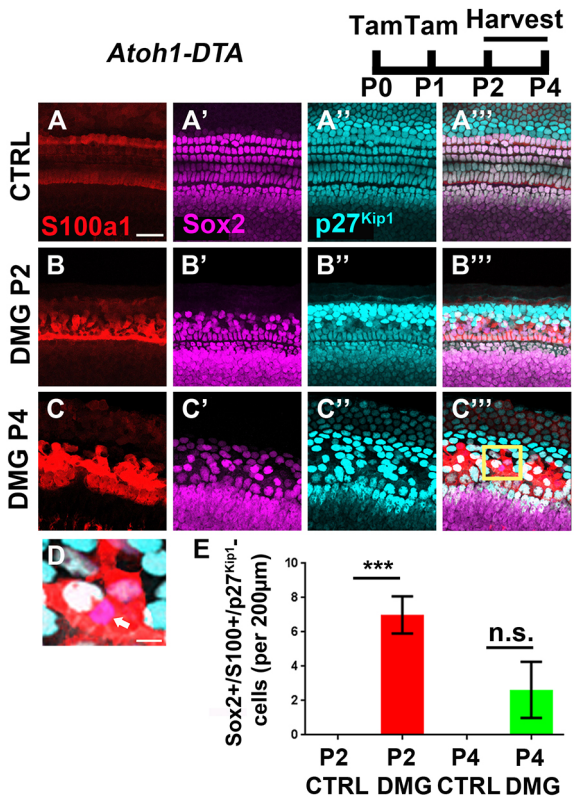

Fig. 6. p27^{Kip1} is specifically downregulated among PCs/DCs during spontaneous HC regeneration in the neonatal mouse cochlea. (A-C‴) Representative confocal slice images with anti-S100a1 (red), anti-Sox2 (magenta), and anti-p27^{Kip1} (cyan) antibodies used to investigate changes in the expression of the cell cycle inhibitor p27^{Kip1} in SCs after HC damage (DMG). Controls (CTRL) for each time point were littermates that lacked either the *Atoh1-CreER^{TM}* or *Rosa26^{DTA}* allele (A-A‴). *Atoh1-DTA* mice were injected with tamoxifen (Tam) at P0/P1 to induce HC death and cochleae were collected at P2 or P4 (B-C‴). All Sox2-positive/p27^{Kip1}-negative cells observed were also S100a1-positive, which suggests that they were PCs and DCs. Scale bar: 25 µm. (D) Higher magnification image of the boxed region in C‴ showing a Sox2-positive/p27^{Kip1}-negative cell (white arrow). Scale bar: 5 µm. (E) A small number of Sox2-positive/S100a1-positive/p27^{Kip1}-negative PCs/DCs were detected at P2 and P4 after HC damage, whereas no p27^{Kip1}-negative cells were detected in controls at any age or outside the S100a1 region. ***P<0.001, determined using a one-way ANOVA with a Sidak's post-hoc test. Data are mean±s.e.m.; n=3-5. n.s., not significant.

GLAST-CreER^{T2}; n=3; Fig. 7B-B‴,D-D‴,F-F‴,H), there were more mitotically regenerated HCs in *Plp-CreER^{T2}* samples that were not fate-mapped (BrdU-positive/tdTomato-negative/myosin VIIa-positive cells; 12.6±1.4 for *Plp-CreER^{T2}* compared with 2.3±1.4 for *Prox1^{CreERT2}* and 2.6±1.4 for *GLAST-CreER^{T2}*; P<0.001; n=3; two-way ANOVA with a Tukey's post-hoc test; Fig. 7G). Therefore, we normalized the number of fate-mapped, mitotically regenerated HCs (BrdU-positive/tdTomato-positive/myosin VIIa-positive cells) to the number of total mitotically regenerated HCs (BrdU-positive/myosin VIIa-positive cells, regardless of tdTomato expression). This ratio showed that 65.8%±18.2% of the mitotically regenerated HCs in *Prox1^{CreERT2}::Rosa26^{tdTomato}::Pou4f3^{DTR}* cochleae were fate-mapped, which was significantly more than the other two lineages (6.2%±6.2% in *Plp-CreER^{T2}* and 5.5%±5.5% in *GLAST-CreER^{T2}*; P<0.05; n=3; two-way ANOVA with a Tukey's post-hoc test; Fig. 7I). This suggests that, although all SC subtypes are equally capable of cell division after HC loss, more PCs and DCs are able to convert into and regenerate HCs after they divide. We then normalized the number of fate-mapped, mitotically regenerated HCs (BrdU-positive/tdTomato-positive/myosin VIIa-positive cells) to the total number of tdTomato-labeled SCs for each CreER line and found no significant difference between *Prox1^{CreERT2}* (0.09%±0.01%), *Plp-CreER^{T2}* (0.09%±0.1%), or *GLAST-CreER^{T2}* (0.02%±0.03%; Fig. 7J). Thus, although the majority of fate-mapped, mitotically regenerated HCs were derived from PCs and DCs, all SC subtypes had the same capacity to divide and remain as SCs, as well as mitotically regenerate HCs.

DISCUSSION

This study investigated the SC subtypes from which HCs spontaneously regenerate within the neonatal mouse cochlea *in vivo*. Previously, Lgr5-positive cells (IPhCs/BCs, inner PCs and the third row of DCs), as well as Hes5-positive cells (some cells of the GER, IPhCs/BCs, outer PCs and DCs) and Sox2-positive cells (cells of the GER, IPhCs/BCs, PCs, DCs and HeCs) were found to regenerate HCs (Bramhall et al., 2014; Cox et al., 2014). Here, we further separated these broad populations of SCs into more discrete groups. Our fate-mapping experiments suggested that PCs, DCs, IPhCs and BCs had the same capacity for regeneration, but that the majority of regenerated HCs were derived from the larger population of PCs and DCs. Furthermore, all fate-mapped SC subtypes had the same capacity for mitotic HC regeneration, although a larger proportion of the BrdU-positive, regenerated HCs were fate-mapped from PCs and DCs than from any other SC subtypes, which is consistent with the location of the p27^{Kip1}-negative cells we observed. These data suggest that PCs, DCs, IPhCs and BCs retain plasticity in the neonatal cochlea, which allows them to spontaneously convert into and regenerate HCs. Unfortunately, none of the CreER lines used here labels 100% of any SC subtype, and a recent paper has shown that Eya1-positive cells in the spiral ganglion region can also act as the source of regenerated HCs (Xu et al., 2017). Therefore fate-mapping quantifications are likely to be an underestimate of the total number of HCs that are regenerated from each population. Nevertheless, the mouse models we used are the best tools currently available for investigating the sources of regenerated HCs.

PCs, DCs, IPhCs and BCs are able to spontaneously regenerate HCs

As the organ of Corti develops, medially located inner HCs differentiate first and therefore they begin to inhibit their neighboring progenitor cells before outer HC differentiation (Driver et al., 2013; Lanford et al., 2000; Morrison et al., 1999). Because of this, laterally located outer HCs and their surrounding SCs may be less mature than their medial counterparts, which could potentially make them more responsive to HC loss. Yet our results suggest that both medial and lateral SC subtypes have equal capacity to form regenerated HCs after damage.

Interestingly, although *GLAST-CreER^{T2}* labels a similar number of IPhCs/BCs (~50-60%) as *Plp-CreER^{T2}*, there was no significant difference in the number of regenerated HCs that were fate-mapped by *GLAST-CreER^{T2}* than in controls without HC damage. IPhCs/BCs are named based on their location within the organ of Corti. Therefore, it is possible that there are two distinct subtypes of IPhCs/BCs that differ in plasticity or in response to HC loss and are differentially fate-mapped by *Plp-CreER^{T2}* versus *GLAST-CreER^{T2}*. Previously, we have shown that *Plp-CreER^{T2}* labels ~6-12% of PCs/DCs (McGovern et al., 2017), which was also observed in the current study. *GLAST-CreER^{T2}*, however, labels <5% of PCs and DCs and, therefore, perhaps the increased

Development (2019) 146, dev171009. doi:10.1242/dev.171009

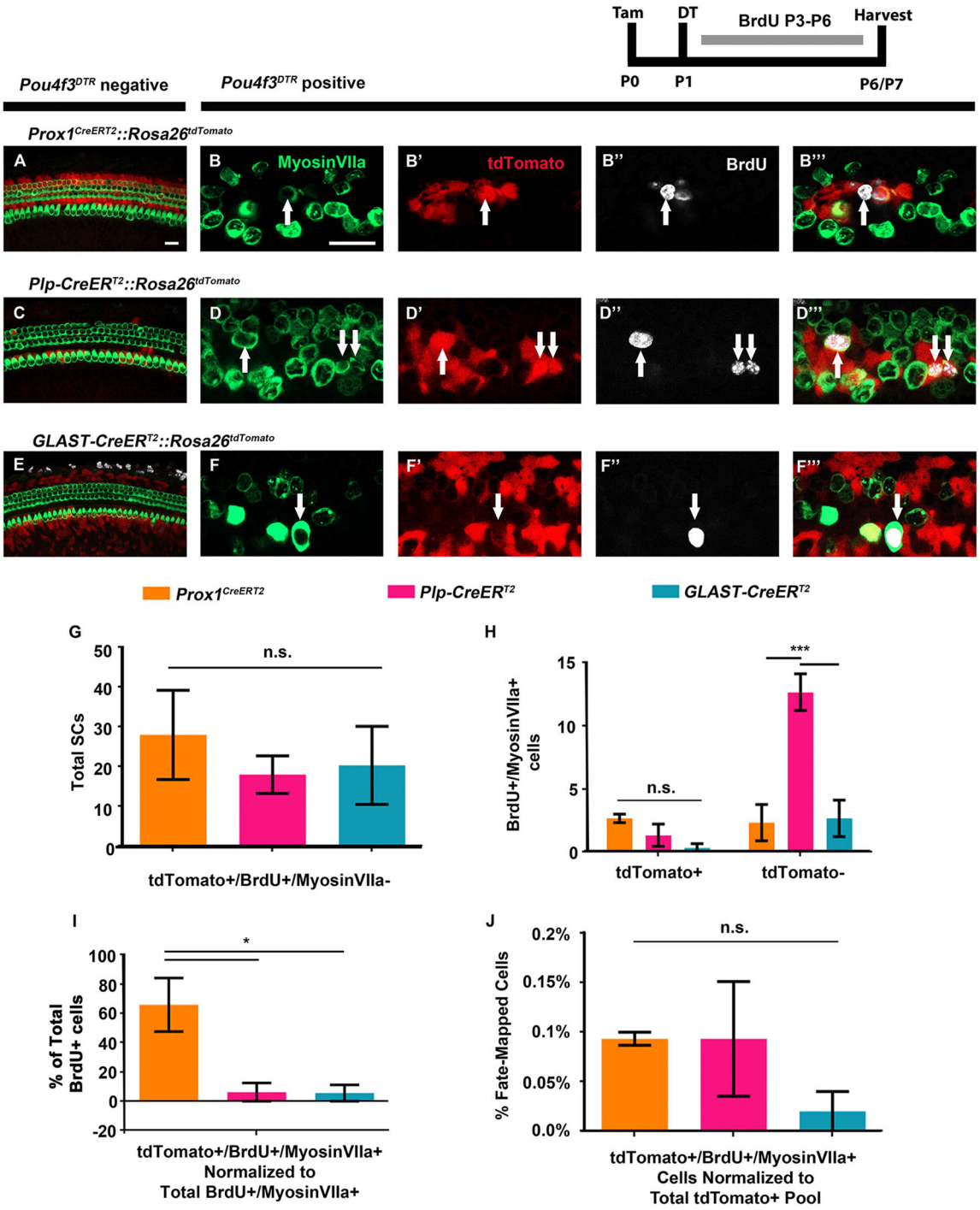

Fig. 7. A larger proportion of mitotically regenerated HCs arise from PCs and DCs. (A-F‴) Representative confocal slice images from P6-P7 *Prox1*^{CreERT2}*::Rosa26*^{tdTomato}*::Pou4f3*^{DTR} (B-B‴), *Plp-CreER*^{T2}*::Rosa26*^{tdTomato}*::Pou4f3*^{DTR} (D-D‴) and *GLAST-CreER*^{T2}*::Rosa26*^{tdTomato}*::Pou4f3*^{DTR} (F-F‴) mice, as well as littermate controls that lacked *Pou4f3*^{DTR} (A,C,E). All mice were injected with tamoxifen (Tam) at P0 to induce tdTomato expression in various SC groups, with diphtheria toxin (DT) at P1 to induce HC death in the experimental samples, and with BrdU twice per day from P3-P6 (~6 h between injections) to detect dividing cells. Samples were immunostained with anti-myosin VIIa antibodies to label HCs (green), anti-BrdU antibodies to label mitotic cells (white) and anti-RFP antibodies to detect tdTomato expression (red). White arrows indicate tdTomato-positive/BrdU-positive/myosin VIIa-positive mitotically regenerated, fate-mapped HCs. Scale bars: 25 µm. (G) No difference was observed in the number of BrdU-positive, fate-mapped SCs that remained as SCs (tdTomato-positive/BrdU-positive/myosin VIIa-negative) among CreER lineages. (H) Significantly more mitotically regenerated HCs that were not fate-mapped (BrdU-positive/myosinVIIA-positive/tdTomato-negative cells) were observed in *Plp-CreER*^{T2}*::Rosa26*^{tdTomato}*::Pou4f3*^{DTR} mice compared with both *Prox1*^{CreERT2} and *GLAST-CreER*^{T2} lineages. However, there was no difference in the number of fate-mapped, mitotically regenerated HCs (BrdU-positive/myosin VIIA-positive/tdTomato-positive cells) among the three lines. (I) When normalized to the total number of BrdU-positive cells, a larger percentage of BrdU-positive/myosin VIIa-positive cells were fate-mapped (tdTomato-positive) by the *Prox1*^{CreERT2} line, compared with *Plp-CreER*^{T2} and *GLAST-CreER*^{T2} lineages. (J) When the total number of fate-mapped mitotically regenerated HCs was normalized to the total number of tdTomato-positive SCs in control cochleae for each CreER line, all groups were found to have an equal capacity for mitotic regeneration. **P*<0.05, ****P*<0.001, determined using two-way ANOVA with a Tukey's post-hoc test. Data are mean±s.e.m.; *n*=3. n.s., not significant.

Development (2019) 146, dev171009. doi:10.1242/dev.171009

amount of labeled PC/DCs contributed to the increased number of regenerated HCs that were observed from the *Plp-CreER^{T2}* lineage.

We have recently shown that increased Notch signaling prevents HC regeneration and that there was no change in *Hes5* expression in IPhCs/BCs in response to HC loss (McGovern et al., 2018). As *Hes5* is a Notch effector and an inhibitor of HC fate (Abdolazimi et al., 2016; Mulvaney and Dabdoub, 2012) we did not predict that regenerated HCs would derive from IPhCs/BCs. However, here we observed a small number of spontaneously regenerated HCs that were fate-mapped from the *Plp-CreER^{T2}* lineage. It is possible that IPhCs/BCs do not rely on HCs for control of *Hes5* expression, as they also have direct contact with inner PCs and cells of the GER that express the Notch ligand jagged 1 (Oesterle et al., 2008; McGovern et al., 2018) or that loss of *Hes5* expression is not necessary for IPhCs/BCs to convert into HCs. It is also possible that the IPhC/BCs that changed cell fate and regenerated HCs are replenished by the cells of the GER as seen previously (Mellado Lagarde et al., 2014). This would limit our ability to detect changes in *Hes5* expression.

In addition, HeCs have been shown to respond to HC damage by invading the damaged outer HC region to remodel and create a scar (Taylor et al., 2012). Although fate-mapping results did not show a significant number of regenerated HCs from HeCs, *GLAST-CreER^{T2}* only labels ∼24% of HeCs throughout the cochlea, with ∼60% of HeCs labeled in the apex. We therefore cannot account for 100% of HeCs, however the majority of HC regeneration occurs in the apical third of the cochlea (Bramhall et al., 2014; Cox et al., 2014) in which the majority of HeCs are labeled. Therefore, we conclude that HeCs do not contribute significantly to spontaneous HC regeneration.

Of note, ototoxic medications and noise-induced hearing loss preferentially damage and kill outer HCs, with little damage inflicted on inner HCs (Nakai et al., 1982; Ou et al., 2000; Williams et al., 1987). Therefore, the finding that PCs and DCs are the source for the majority of spontaneously regenerated HCs is serendipitous, as they are most proximal to the outer HCs that are prone to ototoxic insults. Moreover, studies have shown that some spontaneously regenerated HCs are capable of taking an outer HC fate by expressing prestin (also known as Slc26a5) (Bramhall et al., 2014; Cox et al., 2014). It is still unclear whether spontaneously regenerated HCs are able to adopt an inner HC fate.

Mitotically regenerated HCs predominantly arise from PCs and DCs

Spontaneous HC regeneration is also achieved via mitotic regeneration, in which SCs divide before one or both daughter cells convert into HCs (Cox et al., 2014; Hu et al., 2016). SCs that perform mitotic regeneration are of utmost importance as they have the potential to not only regenerate the HC population, but they can also replenish the SC population, which is necessary for proper cochlear function (Liu et al., 2012b; Mellado Lagarde et al., 2013). The cell cycle inhibitor *p27^{Kip1}* is expressed in cochlear SCs (Chen and Segil, 1999; Lee et al., 2006) and loss of p27^{Kip1} is associated with the ability of isolated SCs to enter the cell cycle before differentiating into HC-like cells (White et al., 2006). In our model of spontaneous HC regeneration, a small number of PCs and DCs lost p27^{Kip1} expression after HC damage. Fate-mapping studies combined with the mitotic tracer BrdU revealed that, whereas all groups of SCs were able to divide and remain as SCs, as well as to mitotically regenerate HCs at the same rate, a larger proportion of mitotically regenerated HCs were fate-mapped by *Prox1^{CreERT2}* and therefore were derived from PCs/DCs. Although we investigated the expression of p27^{Kip1} in this study, it is not the only cell cycle regulator that is expressed in the developing mammalian cochlea. *p19^{Ink4d}* and *p21^{Cip1}* have been shown to inhibit cell cycle re-entry of cochlear cells (Laine et al., 2007); however the role of these cell cycle regulators in the postnatal cochlea is not well understood. Therefore, *p19^{Ink4d}* and *p21^{Cip1}* may regulate the ability of other SC subtypes to divide.

Because BrdU incorporates into cells during S phase of the cell cycle (Miller and Nowakowski, 1988) and has an estimated bioavailability of ∼15-30 min after injection in mice (Burns et al., 2012; Mandyam et al., 2007), it is very likely that we are underestimating the number of mitotically regenerated HCs. However, measuring the ratio of fate-mapped, mitotically regenerated HCs to the total number of mitotically regenerated HCs can partially account for the different number of BrdU-positive cells observed between samples because within the same cochlea, all cells have access to BrdU at the same time. Additionally, while significantly more mitotically regenerated HCs were formed in cochleae from *Plp-CreER^{T2}* mice, only a small number of these cells were fate-mapped. This indicates that SC subtypes other than IPhCs/BCs are mitotically regenerating HCs in the *Plp-CreER^{T2}* samples and supports our conclusion that PCs/DCs contribute a larger proportion of mitotically regenerated HCs. Yet when the fate-mapped, mitotically regenerated HCs were normalized to the total number of fate-mapped cells in each CreER line, all SC subtypes had the same capacity to produce mitotically regenerated HCs.

The source for spontaneous HC regeneration is not limited to Lgr5-positive SCs

It has been hypothesized that Wnt-responsive Lgr5-positive cells (IPhCs/BCs, inner PCs and the third row of DCs) within the neonatal organ of Corti are the cochlear stem cells from which HCs are regenerated (Bramhall et al., 2014; Chai et al., 2012; McLean et al., 2017; Shi et al., 2012; Shi et al., 2013; Waqas et al., 2016). Wnt signaling has been suggested as the mechanism that drives proliferation of SCs in the developing cochlea (Chai et al., 2012; Ni et al., 2016a,b; Hu et al., 2016; Shi et al., 2013; Kuo et al., 2015). In addition, the interaction of Wnt and Notch signaling has been implicated in the ability of SCs to divide and then transdifferentiate into HCs (Hu et al., 2016; Li et al., 2015; Ni et al., 2016a,b; Shi et al., 2013; Wang et al., 2015). The majority of these studies used isolated Lgr5-positive cells grown in culture, or undamaged cochleae treated with Wnt agonists or prolonged expression of the Wnt effector β-catenin to make their conclusions. While these studies nicely demonstrate that Lgr5-positive cells are responsive to Wnt signaling and can divide or produce new HCs when Wnt signaling is activated, they do not address the question of which SC subtypes are the source of regenerated HCs that form spontaneously in the neonatal cochlea.

There are two studies that directly investigate this question. The first study that investigated the contribution of Lgr5-positive cells to spontaneous HC regeneration (Bramhall et al., 2014) had several limitations, which cloud the interpretations that can be made from the data. Specifically, explant cultures from the neonatal cochlea were used to investigate spontaneous HC regeneration in response to gentamycin ototoxicity. This system is problematic because the majority of HC regeneration is seen in the apical third of the cochlea (Cox et al., 2014; McGovern et al., 2018) and the apex is resistant to gentamycin-induced damage in the neonate (Chen et al., 2009; Korrapati et al., 2013). Therefore, less HC regeneration occurs in explants compared with HC damage that is induced with mouse genetics *in vivo*. Secondly, the conclusion that more regenerated

Development (2019) 146, dev171009. doi:10.1242/dev.171009

HCs were derived from the Lgr5-population was made by comparing the number of regenerated HCs fate-mapped by *Lgr5*^{CreER} versus *Sox2*^{CreER}. Fate-mapping SCs in the neonatal cochlea with *Sox2*^{CreER} is challenging to interpret because it induces recombination in a large number of HCs as well as in SCs (McGovern et al., 2017; Walters et al., 2015). Furthermore, *Sox2*^{CreER} was recently shown to have a ∼30% reduction in *Sox2* expression, which generates a haploinsufficent phenotype. *Sox2*^{CreER} mice have increased proliferation of neonatal SCs in samples without HC damage, increased proliferation and formation of regenerated HCs after damage, and increased response to Wnt signaling (Atkinson et al., 2018). Therefore, conclusions about the source of regenerated HCs are not clear in this study.

In the second study, ∼123 spontaneously regenerated HCs were fate-mapped from the Lgr5 population in which the authors used the same *Pou4f3*^{DTR} mouse model of HC damage, the same tdTomato reporter line, induced HC damage at P1 with the same dose of DT, and collected the tissue at the same age of P7 (Cox et al., 2014). However, in the present study we only detected ∼50 regenerated HCs fate-mapped from the Prox1 population. This difference may indicate that Lgr5-positive cells produce even more regenerated HCs than PCs and DCs, or there may have been different amounts of HC damage in the two studies, which triggered different amounts of regeneration. In support of the latter conclusion, we also detected ∼44% fewer Sox2/myosin VIIa double positive HCs compared with Cox et al. (2014) which suggests that there was less regeneration occurring in our study. Because DT is a protein that may degrade quickly and the dose injected is very small (6.25 ng/g), different amounts of HC damage induced by DT injection could vary from lab to lab. Additionally, *Prox1*^{CreERT2} only labels ∼30% of inner PCs whereas *Lgr5*^{CreERT2} labels ∼67% of inner PCs (Cox et al., 2014); thus, if inner PCs are a significant contributor to regeneration, the difference in inner PC fate-mapping may account for the increased numbers of regenerated HCs seen with *Lgr5*^{CreERT2}. Unfortunately, there are no inner PC-specific CreER lines available to address this issue.

Throughout late embryonic and neonatal development of the murine cochlea, cellular changes occur rapidly to downregulate the expression of progenitor cell genes, while upregulating the expression of genes that drive terminal differentiation. Specifically, during the first postnatal week, the expression of genes in the Notch signaling pathway is decreasing, whereas the expression of genes that determine inner and outer HC fate is increasing (Abe et al., 2007; Belyantseva et al., 2000; Hartman et al., 2007; Legendre et al., 2008; Maass et al., 2015; Maass et al., 2016; Murata et al., 2006; Zheng et al., 2000). Because there are different gene expression changes happening in different SC subtypes within the neonatal cochlea, understanding which SC subtypes retain plasticity when HC regeneration occurs spontaneously will narrow the scope of investigation to identify barriers to HC regeneration in the more mature cochlea. We have identified PCs, DCs, IPhCs and BCs as the source for spontaneous HC regeneration, which suggests that they remain plastic longer than other SC subtypes. Therefore, investigating changes that occur during the first postnatal week in these cells may lead to the discovery of therapeutic targets to treat hearing loss.

MATERIALS AND METHODS

Animals

GLAST-CreER^{T2} mice (stock #12586, Wang et al., 2012); *Plp-CreER*^{T2} mice (stock #5975, Doerflinger et al., 2003); *Rosa26*^{tdTomato} mice, also referred to as Ai14 (stock #7914, Madisen et al., 2010); and *Rosa26*$^{loxP\text{-}stop\text{-}loxP\text{-}DTA}$ mice (stock #6331, Ivanova et al., 2005) were obtained from The Jackson Laboratory. *Atoh1-CreER*^{TM} mice (Chow et al., 2006) were provided by Dr Suzy Baker (St Jude Children's Hospital, Memphis, TN, USA), *Pou4f3*^{DTR} mice (Golub et al., 2012; Tong et al., 2015) were provided by Dr Ed Rubel (University of Washington, Seattle, WA, USA), and *Prox1*^{CreERT2} mice (Srinivasan et al., 2007) were provided by Dr Guillermo Oliver (St Jude Children's Research Hospital, Memphis, TN, USA). Transnetyx, Inc. performed all genotyping. Mice of both genders were used and all animal work was performed in accordance with approved animal protocols from the Institutional Animal Care and Use Committee at Southern Illinois University School of Medicine.

Substances given to animals

To induce HC death in *Atoh1-DTA* mice, tamoxifen (Sigma-Aldrich) was dissolved in 100% corn oil and injected IP at 3 mg/40 g on P0 and P1. For fate-mapping experiments, tamoxifen (3 mg/40 g) was injected IP at P0 only to induce tdTomato expression in SC subgroups, followed by injection of DT (6.25 ng/g, IM; List Biological Laboratories, Inc.) at P1 to induce HC death in *Pou4f3*^{DTR} mice. For investigation of mitotic cells, BrdU (Sigma-Aldrich) was injected (50 mg/kg, IP) from P3-P6 twice a day (with ∼6 h between injections) in addition to the tamoxifen and DT injections at P0 and P1, respectively.

Immunostaining

Neonatal pups were euthanized under isoflurane anesthesia and cochleae were collected and post-fixed in 4% paraformaldehyde (Polysciences, Inc.) for ∼2 h at room temperature. The samples were then transferred to 10 mM PBS (Sigma-Aldrich) and stored at 4°C. Following whole-mount dissection, the cochlea was cut into three turns of equal length and placed into a 48-well plate for immunostaining as described previously (McGovern et al., 2018).

The primary antibodies used in this study are listed in Table S1, along with the additional steps to the immunostaining protocol needed for some antibodies. A low pH antigen unmasking solution (AUM, Vector Laboratories) was beneficial to increase antibody binding to the epitope. For this step, samples were incubated in a hybridization oven at 95°C for 45 min with a 1:100 dilution of the AUM solution in ddH_2O followed by three 5 min washes in 10 mM PBS before blocking/permeabilization. In addition, some antibodies produced excessive background and, therefore, to increase the signal to noise ratio, Image-iT^{TM} FX signal enhancer (enough volume to cover each sample, Life Technologies) was applied at room temperature for 30 min followed by three 5 min PBS washes prior to the blocking/permeabilization step. If used in combination with the AUM step, signal enhancer was added just before the blocking/permeabilization step. To investigate mitotic activity within the cochlea, samples that had been injected with BrdU were incubated with HCl to open the DNA and allow anti-BrdU antibodies to penetrate. After the secondary antibody (Table S2) step was completed for all other targets, samples were incubated with 2N HCl (Fisher Scientific International) at 37°C for 25 min followed by three washes with 0.1 M Tris-HCL (Fisher Scientific International) for 5 min each, and an overnight incubation with the Alexa fluor-conjugated BrdU primary antibody at 4°C. The HCl incubation step destroys endogenous tdTomato fluorescence; therefore anti-RFP antibodies were used in samples that were injected with BrdU. Mouse monoclonal p27^{Kip1} antibodies and RFP antibodies were used in combination with IgG-specific secondary antibodies to increase specific binding.

Cell counts

Imaging was conducted using a Leica SP5 or a Zeiss LSM 800 confocal microscope and images were processed with LAS-lite (Leica) or Zen Blue lite (Zeiss) software. Because the majority of HC regeneration occurs in the apical third of the neonatal mouse cochlea, quantification of Sox2-positive HCs and p27^{Kip1}-negative cells was conducted only in the apex. For quantification of Sox2-positive HCs, the whole apical turn was imaged and counted. For quantification of p27^{Kip1}-negative cells, images were taken from two representative regions in the apical turn of the cochlea and a 200 µm region per image was quantified and averaged for each sample. For fate-mapping experiments, the entire cochlea was imaged and divided into six

segments of equal length as previously described (McGovern et al., 2017). The total number of tdTomato/myosin VIIa double positive cells was quantified in each segment of the cochlea. For BrdU quantification, tdTomato-positive/myosin VIIa-positive/BrdU-positive, tdTomato-negative/myosin VIIa-positive/BrdU-positive, as well as tdTomato-positive/myosin VIIa-negative/BrdU-positive cells were counted in the entire cochlea. Similar to McGovern et al. (2018), in order to separate the cells of the GER from IPhC/BCs, the width of the tdTomato-positive region medial to inner HCs in *Plp-CreER^{T2}::Rosa26^{tdTomato}* cochleae was measured and used to define the Sox2-positive IPhCs/BCs in *Glast-CreER^{T2}* samples. The Sox2-positive cells medial to this region were considered to be the cells of the GER.

Normalization of HC damage and regeneration across CreER lines

We first quantified the number of myosin VIIa-positive HCs in two representative 200 µm regions per cochlear turn in undamaged controls as well as in samples with HC damage and regeneration. We then calculated a ratio of the number of myosin VIIa-positive cells in HC-damaged samples to the number of myosin VIIa-positive cells in undamaged samples. If all groups had the same level of HC damage and regeneration, the number of surviving HCs plus the number of regenerated HCs across samples should remain consistent among CreER lines.

As a second metric for the level of spontaneous HC regeneration, we counted the number of Sox2-positive HCs at P7 in each of the CreER lines. Although Sox2-positive HCs at P7 do not represent the total number of regenerated HCs, the number of Sox2-positive cells should be consistent at P7 across all CreER lines if the level of regeneration is similar. Other studies have used this metric to quantify HC regeneration (Bramhall et al., 2014; Cox et al., 2014; Kempfle et al., 2016; McLean et al., 2017). Because the majority of HC regeneration occurs in the apical third of the neonatal cochlea, quantification was limited to this region.

Normalization of SCs labeled by each CreER line to determine regeneration capacity

To generate the total number of tdTomato-positive SCs for each CreER line, we determined the number of Sox2-positive SCs and the percentage of tdTomato-positive/Sox2-positive SC in a 200 µm region in each turn of the cochlea. We then calculated the average number of Sox2-positive SCs present in the entire cochlea by dividing the length of each cochlea by 200 µm and multiplying that number by the number of Sox2-positive cells per 200 µm. This gave us the total number of Sox2-positive cells within the cochlea. We calculated the total number of tdTomato-positive cells labeled by each CreER line by multiplying the total Sox2-positive pool with the percent of SCs expressing tdTomato. We then generated a percentage by dividing the number of tdTomato/myosin VIIa double positive cells in samples with HC damage by the total number of tdTomato-positive cells labeled by each CreER line.

Statistical analysis

All data are mean±s.e.m. and the *n* value represents the number of mice included in the study in which one cochlea from each mouse was used for a particular experiment. Statistical tests used for each dataset are described in the results text and figure legends and analyses were performed using Graphpad Prism 6.02.

Acknowledgements

We thank Dr Brad Walters from University of Mississippi Medical Center and Dr Andy Groves from Baylor College of Medicine for critical discussion. *Atoh1-CreER^{TM}*, *Pou4f3^{DTR}* and *Prox1^{CreERT2}* mice were kind gifts from Dr Suzanne Baker at St. Jude Children's Research Hospital, Dr Ed Rubel at the University of Washington and Dr Guillermo Oliver at St. Jude Children's Research Hospital, respectively.
The Southern Illinois University School of Medicine Research Imaging Facility is supported by a grant from the Office of Naval Research (N00014-15-1-2866) and the National Center for Research Resources – Health (S10RR027716).

Competing interests

B.C.C. is a consultant for Turner Scientific and Otonomy. M.R.R. is a part-time employee for Turner Scientific.

Author contributions

Conceptualization: M.M.M., B.C.C.; Methodology: M.M.M., B.C.C.; Validation: M.M.M.; Formal analysis: M.M.M., B.C.C.; Investigation: M.M.M., M.R.R., C.L.C., K.A.G.; Writing - original draft: M.M.M., B.C.C.; Writing - review & editing: M.M.M., M.R.R., K.A.G., B.C.C.; Visualization: M.M.M., M.R.R., K.A.G.; Supervision: B.C.C.; Project administration: M.M.M., B.C.C.; Funding acquisition: B.C.C.

Funding

This work was supported by the National Institutes of Health (R01 DC014441) and the Office of the Assistant Secretary for Health (W81XWH-15-1-0475). Deposited in PMC for release after 12 months.

Supplementary material

Supplementary material available online at
http://dev.biologists.org/lookup/doi/10.1242/dev.171009.supplemental

References

Abdolazimi, Y., Stojanova, Z. and Segil, N. (2016). Selection of cell fate in the organ of Corti involves the integration of Hes/Hey signaling at the Atoh1 promoter. *Development* **143**, 841-850.
Abe, T., Kakehata, S., Kitani, R., Maruya, S. I., Navaratnam, D., Santos-Sacchi, J. and Shinkawa, H. (2007). Developmental expression of the outer hair cell motor prestin in the mouse. *J. Membr. Biol.* **215**, 49-56.
Abrahamsen, B., Zhao, J., Asante, C. O., Cendan, C. M., Marsh, S., Martinez-Barbera, J. P., Nassar, M. A., Dickenson, A. H. and Wood, J. N. (2008). The cell and molecular basis of mechanical, cold, and inflammatory pain. *Science* **321**, 702-705.
Abrashkin, K. A., Izumikawa, M., Miyazawa, T., Wang, C.-H., Crumling, M. A., Swiderski, D. L., Beyer, L. A., Gong, T. W. L. and Raphael, Y. (2006). The fate of outer hair cells after acoustic or ototoxic insults. *Hear. Res.* **218**, 20-29.
Anttonen, T., Belevich, I., Kirjavainen, A., Laos, M., Brakebusch, C., Jokitalo, E. and Pirvola, U. (2014). How to bury the dead: elimination of apoptotic hair cells from the hearing organ of the mouse. *J. Assoc. Res. Otolaryngol.* **15**, 975-992.
Atkinson, P. J., Dong, Y., Gu, S., Liu, W., Najarro, E. H., Udagawa, T. and Cheng, A. G. (2018). Sox2 haploinsufficiency primes regeneration and Wnt responsiveness in the mouse cochlea. *J. Clin. Invest.* **128**, 1641-1656.
Balak, K. J., Corwin, J. T. and Jones, J. E. (1990). Regenerated hair cells can originate from supporting cell progeny: evidence from phototoxicity and laser ablation experiments in the lateral line system. *J. Neurosci.* **10**, 2502-2512.
Basch, M. L., Brown, R. M., Jen, H.-I. and Groves, A. K. (2016). Where hearing starts: The development of the mammalian cochlea. *J. Anat.* **228**, 233-254.
Belyantseva, I. A., Adler, H. J., Curi, R., Frolenkov, G. I. and Kachar, B. (2000). Expression and localization of prestin and the sugar transporter GLUT-5 during development of electromotility in cochlear outer hair cells. *J. Neurosci.* **20**, RC116.
Bohne, B. A. (1976). Safe level for noise exposure? *Ann. Otol. Rhinol. Laryngol.* **85**, 711-724.
Bramhall, N. F., Shi, F., Arnold, K., Hochedlinger, K. and Edge, A. S. B. (2014). Lgr5-positive supporting cells generate new hair cells in the postnatal cochlea. *Stem Cell Rep.* **2**, 311-322.
Burns, J. C., On, D., Baker, W., Collado, M. S. and Corwin, J. T. (2012). Over half the hair cells in the mouse utricle first appear after birth, with significant numbers originating from early postnatal mitotic production in peripheral and striolar growth zones. *J. Assoc. Res. Otolaryngol.* **13**, 609-627.
Chai, R., Xia, A., Wang, T., Jan, T. A., Hayashi, T., Bermingham-McDonogh, O. and Cheng, A. G. L. (2011). Dynamic expression of Lgr5, a Wnt target gene, in the developing and mature mouse cochlea. *J. Assoc. Res. Otolaryngol.* **12**, 455-469.
Chai, R., Kuo, B., Wang, T., Liaw, E. J., Xia, A., Jan, T. A., Liu, Z., Taketo, M. M., Oghalai, J. S., Nusse, R. et al. (2012). Wnt signaling induces proliferation of sensory precursors in the postnatal mouse cochlea. *Proc. Natl. Acad. Sci. USA* **109**, 8167-8172.
Chen, P. and Segil, N. (1999). p27(Kip1) links cell proliferation to morphogenesis in the developing organ of Corti. *Development* **126**, 1581-1590.
Chen, F.-Q., Schacht, J. and Sha, S. (2009). Aminoglycoside-induced histone deacetylation and hair cell death in the mouse cochlea. *J. Neurochem.* **108**, 1226-1236.
Chow, L. M. L., Tian, Y., Weber, T., Corbett, M., Zuo, J. and Baker, S. J. (2006). Inducible Cre recombinase activity in mouse cerebellar granule cell precursors and inner ear hair cells. *Dev. Dyn.* **235**, 2991-2998.
Corwin, J. T. and Cotanche, D. A. (1988). Regeneration of sensory hair cells after acoustic trauma. *Science* **240**, 1772-1774.
Cox, B. C., Liu, Z., Lagarde, M. M. M. and Zuo, J. (2012). Conditional gene expression in the mouse inner ear using cre-loxP. *J. Assoc. Res. Otolaryngol.* **13**, 295-322.
Cox, B. C., Chai, R., Lenoir, A., Liu, Z., Zhang, L., Nguyen, D.-H., Chalasani, K., Steigelman, K. A., Fang, J., Rubel, E. W. et al. (2014). Spontaneous hair

cell regeneration in the neonatal mouse cochlea in vivo. *Development* **141**, 816-829.
Dabdoub, A., Puligilla, C., Jones, J. M., Fritzsch, B., Cheah, K. S. E., Pevny, L. H. and Kelley, M. W. (2008). Sox2 signaling in prosensory domain specification and subsequent hair cell differentiation in the developing cochlea. *Proc. Natl. Acad. Sci. USA* **105**, 18396-18401.
Doerflinger, N., Macklin, W. and Popko, B. (2003). Inducible site-specific recombination in myelinating cells. *Genesis* **35**, 63-72.
Driver, E. C., Sillers, L., Coate, T. M., Rose, M. F. and Kelley, M. W. (2013). The Atoh1-lineage gives rise to hair cells and supporting cells within the mammalian cochlea. *Dev. Biol.* **376**, 86-98.
Flores-Otero, J., Xue, H. Z. and Davis, R. L. (2007). Reciprocal regulation of presynaptic and postsynaptic proteins in bipolar spiral ganglion neurons by neurotrophins. *J. Neurosci.* **27**, 14023-14034.
Furness, D. N., Hulme, J. A., Lawton, D. and Hackney, C. M. (2002). Distribution of the glutamate/aspartate transporter GLAST in relation to the afferent synapses of outer hair cells in the guinea pig cochlea. *J. Assoc. Res. Otolaryngol.* **3**, 234-247.
Golub, J. J. S., Tong, L., Ngyuen, T. B., Hume, C. R., Palmiter, R. D., Rubel, E. W. and Stone, J. S. (2012). Hair cell replacement in adult mouse utricles after targeted ablation of hair cells with diphtheria toxin. *J. Neurosci.* **32**, 15093-15105.
Gómez-Casati, M. E., Murtie, J. C., Rio, C., Stankovic, K., Liberman, M. C. and Corfas, G. (2010a). Nonneuronal cells regulate synapse formation in the vestibular sensory epithelium via erbB-dependent BDNF expression. *Proc. Natl. Acad. Sci. USA* **107**, 17005-17010.
Gómez-Casati, M. M. E., Murtie, J., Taylor, B. and Corfas, G. (2010b). Cell-specific inducible gene recombination in postnatal inner ear supporting cells and glia. *J. Assoc. Res. Otolaryngol.* **11**, 19-26.
Hartman, B. H., Hayashi, T., Nelson, B. R., Bermingham-McDonogh, O. and Reh, T. A. (2007). Dll3 is expressed in developing hair cells in the mammalian cochlea. *Dev. Dyn.* **236**, 2875-2883.
Hawkins, J. E., Johnsson, L. G., Stebbins, W. C., Moody, D. B. and Coombs, S. L. (1976). Hearing loss and cochlear pathology in monkeys after noise exposure. *Acta Otolaryngol.* **81**, 337-343.
Hu, L., Lu, J., Chiang, H., Wu, H., Edge, A. S. B. and Shi, F. (2016). Diphtheria toxin-induced cell death triggers wnt-dependent hair cell regeneration in neonatal mice. *J. Neurosci.* **36**, 9479-9489.
Hume, C. R., Bratt, D. L. and Oesterle, E. C. (2007). Expression of LHX3 and SOX2 during mouse inner ear development. *Gene Expr. Patterns* **7**, 798-807.
Ivanova, A., Signore, M., Caro, N., Greene, N. D. E., Copp, A. J. and Martinez-Barbera, J. P. (2005). In vivo genetic ablation by Cre-mediated expression of diphtheria toxin fragment A. *Genesis* **43**, 129-135.
Jahan, I., Pan, N., Elliott, K. L. and Fritzsch, B. (2015). The quest for restoring hearing: understanding ear development more completely. *BioEssays* **37**, 1016-1027.
Jones, J. E. and Corwin, J. T. (1996). Regeneration of sensory cells after laser ablation in the lateral line system: hair cell lineage and macrophage behavior revealed by time-lapse video microscopy. *J. Neurosci.* **16**, 649-662.
Kempfle, J. S., Turban, J. L. and Edge, A. S. B. (2016). Sox2 in the differentiation of cochlear progenitor cells. *Sci. Rep.* **6**, 23293.
Kiernan, A. E., Cordes, R., Kopan, R., Gossler, A. and Gridley, T. (2005). The Notch ligands DLL1 and JAG2 act synergistically to regulate hair cell development in the mammalian inner ear. *Development* **132**, 4353-4362.
Kikuchi, T., Adams, J. C., Miyabe, Y., So, E. and Kobayashi, T. (2000). Potassium ion recycling pathway via gap junction systems in the mammalian cochlea and its interruption in hereditary nonsyndromic deafness. *Med. Electron Microsc.* **33**, 51-56.
Korrapati, S., Roux, I., Glowatzki, E. and Doetzlhofer, A. (2013). Notch signaling limits supporting cell plasticity in the hair cell-damaged early postnatal murine cochlea. *PLoS One* **8**, e7327.
Kuo, B. R., Baldwin, E. M., Layman, W. S., Taketo, M. M., and Zuo, J. (2015). In vivo cochlear hair cell generation and survival by coactivation of β-catenin and Atoh1. *J. Neurosci.* **35**, 10786-10798.
Laine, H., Doetzlhofer, A., Mantela, J., Ylikoski, J., Laiho, M., Roussel, M. F., Segil, N. and Pirvola, U. (2007). p19Ink4d and p21Cip1 collaborate to maintain the postmitotic state of auditory hair cells, their codeletion leading to DNA damage and p53-mediated apoptosis. *J. Neurosci.* **27**, 1434-1444.
Lanford, P. J., Shailam, R., Norton, C. R., Ridley, T. and Kelley, M. W. (2000). Expression of Math1 and HES5 in the cochleae of wildtype and Jag2 mutant mice. *J. Assoc. Res. Otolaryngol.* **1**, 161-171.
Lee, Y. Y.-S., Liu, F. and Segil, N. (2006). A morphogenetic wave of p27Kip1 transcription directs cell cycle exit during organ of Corti development. *Development* **133**, 2817-2826.
Legendre, K., Safieddine, S., Kussel-Andermann, P., Petit, C. and El-Amraoui, A. (2008). II- V spectrin bridges the plasma membrane and cortical lattice in the lateral wall of the auditory outer hair cells. *J. Cell Sci.* **121**, 3347-3356.
Li, W., Wu, J., Yang, J., Sun, S., Chai, R., Chen, Z.-Y. and Li, H. (2015). Notch inhibition induces mitotically generated hair cells in mammalian cochleae via activating the Wnt pathway. *Proc. Natl. Acad. Sci.* **112**, 166-171.
Liu, Z., Dearman, J. A., Cox, B. C., Walters, B. J., Zhang, L., Ayrault, O., Zindy, F., Gan, L., Roussel, M. F. and Zuo, J. (2012a). Age-dependent in vivo conversion of mouse cochlear pillar and Deiters' cells to immature hair cells by Atoh1 ectopic expression. *J. Neurosci.* **32**, 6600-6610.
Liu, Z., Walters, B. J., Owen, T., Brimble, M. A., Steigelman, K. A., Zhang, L., Lagarde, M. M. M., Valentine, M. B., Yu, Y., Cox, B. C. et al. (2012b). Regulation of p27Kip1 by Sox2 maintains quiescence of inner pillar cells in the murine auditory sensory epithelium. *J. Neurosci.* **32**, 10530-10540.
Liu, Z., Fang, J., Dearman, J., Zhang, L. and Zuo, J. (2014). In vivo generation of immature inner hair cells in neonatal mouse cochleae by ectopic Atoh1 expression. *PLoS One* **9**, e89377.
Maass, J. C., Gu, R., Basch, M. L., Waldhaus, J., Lopez, E. M., Xia, A., Oghalai, J. S., Heller, S. and Groves, A. K. (2015). Changes in the regulation of the Notch signaling pathway are temporally correlated with regenerative failure in the mouse cochlea. *Front. Cell. Neurosci.* **9**, 110.
Maass, J. C., Gu, R., Cai, T., Wan, Y.-W., Cantellano, S. C., Asprer, J. S. T., Zhang, H., Jen, H.-I., Edlund, R. K., Liu, Z. et al. (2016). Transcriptomic analysis of mouse cochlear supporting cell maturation reveals large-scale changes in Notch responsiveness prior to the onset of hearing. *PLoS One* **11**, e0167286.
Madisen, L., Zwingman, T. A., Sunkin, S. M., Oh, S. W., Zariwala, H. A., Gu, H., Ng, L. L., Palmiter, R. D., Hawrylycz, M. J., Jones, A. R. et al. (2010). A robust and high-throughput Cre reporting and characterization system for the whole mouse brain. *Nat. Neurosci.* **13**, 133-140.
Mak, A. C. Y., Szeto, I. Y. Y., Fritzsch, B. and Cheah, K. S. E. (2009). Differential and overlapping expression pattern of SOX2 and SOX9 in inner ear development. *Gene Expr. Patterns* **9**, 444-453.
Mandyam, C. D., Harburg, G. C. and Eisch, A. J. (2007). Determination of key aspects of precursor cell proliferation, cell cycle length and kinetics in the adult mouse subgranular zone. *Neuroscience* **146**, 108-122.
McGovern, M. M., Brancheck, J., Grant, A. C., Graves, K. A. and Cox, B. C. (2017). Quantitative analysis of supporting cell subtype labeling among CreER lines in the neonatal mouse cochlea. *J. Assoc. Res. Otolaryngol.* **18**, 227-245.
McGovern, M. M., Zhou, L., Randle, M. R. and Cox, B. C. (2018). Spontaneous hair cell regeneration is prevented by increased notch signaling in supporting cells. *Front. Cell. Neurosci.* **12**, 120.
McLean, W. J., Yin, X., Lu, L., Lenz, D. R., McLean, D., Langer, R., Karp, J. M. and Edge, A. S. B. (2017). Clonal expansion of lgr5-positive cells from mammalian cochlea and high-purity generation of sensory hair cells. *Cell Rep.* **18**, 1917-1929.
Mellado Lagarde, M. M., Cox, B. C., Fang, J., Taylor, R., Forge, A. and Zuo, J. (2013). Selective ablation of pillar and deiters' cells severely affects cochlear postnatal development and hearing in mice. *J. Neurosci.* **33**, 1564-1576.
Mellado Lagarde, M. M., Wan, G., Zhang, L., Gigliello, A. R., McInnis, J. J., Zhang, Y., Bergles, D., Zuo, J., Corfas, G., Snyder, S. H. et al. (2014). Spontaneous regeneration of cochlear supporting cells after neonatal ablation ensures hearing in the adult mouse. *Proc. Natl. Acad. Sci. USA* **111**, 16919-16924.
Miller, M. W. and Nowakowski, R. S. (1988). Use of bromodeoxyuridine-immunohistochemistry to examine the proliferation, migration and time of origin of cells in the central nervous system. *Brain Res.* **457**, 44-52.
Morrison, A., Hodgetts, C., Gossler, A., Hrabé De Angelis, M. and Lewis, J. (1999). Expression of Delta1 and Serrate1 (Jagged 1) in the mouse inner ear. *Mech. Dev.* **84**, 169-172.
Mulvaney, J. and Dabdoub, A. (2012). Atoh1, an essential transcription factor in neurogenesis and intestinal and inner ear development: Function, regulation, and context dependency. *J. Assoc. Res. Otolaryngol.* **13**, 281-293.
Murata, J., Tokunaga, A., Okano, H. and Kubo, T. (2006). Mapping of Notch activation during cochlear development in mice: Implications for determination of prosensory domain and cell fate diversification. *J. Comp. Neurol.* **497**, 502-518.
Nakai, Y., Konishi, K., Chang, K. C., Ohashi, K., Morisaki, N., Minowa, Y. and Morimoto, A. (1982). Ototoxicity of the anticancer drug cisplatin. An experimental study. *Acta Otolaryngol.* **93**, 227-232.
Ni, W., Zeng, S., Li, W., Chen, Y., Zhang, S., Tang, M., Sun, S., Chai, R. and Li, H. (2016a). Wnt activation followed by Notch inhibition promotes mitotic hair cell regeneration in the postnatal mouse cochlea. *Oncotarget* **7**, 66754-66768.
Ni, W., Lin, C., Guo, L., Wu, K., Chen, Y., Chair, R., Li, W. and Li, H. (2016b). Extensive supporting cell proliferation and mitotic hair cell generation by in vivo genetic reprogramming in the neonatal mouse cochlea. *J. Neuorsci.* **36**, 8734-8745.
Oesterle, E. C., Campbell, S., Taylor, R. R., Forge, A. and Hume, C. R. (2008). Sox2 and Jagged1 expression in normal and drug-damaged adult mouse inner ear. *J. Assoc. Res. Otolaryngol.* **9**, 65-89.
Oesterle, E. C., Chien, W. M., Campbell, S., Nellimarla, P. and Fero, M. L. (2011). p27Kip1 is required to maintain proliferative quiescence in the adult cochlea and pituitary. *Cell Cycle* **10**, 1237-1248.
Ou, H. C., Bohne, B. A. and Harding, G. W. (2000). Noise damage in the C57BL/CBA mouse cochlea. *Hear. Res.* **145**, 111-122.
Raphael, Y. and Altschuler, R. A. (2003). Structure and innervation of the cochlea. *Brain Res. Bull.* **60**, 397-422.

Rubel, E. W., Furrer, S. A. and Stone, J. S. (2013). A brief history of hair cell regeneration research and speculations on the future. *Hear. Res.* **297**, 42-51.
Ryals, B. and Rubel, E. W. (1988). Ryals 1988 Hair cell regeneration after acoustic trauma in adult Coturnix quail. *Science.* **240**, 1774-1776.
Shang, J., Cafaro, J., Nehmer, R. and Stone, J. (2010). Supporting cell division is not required for regeneration of auditory hair cells after ototoxic injury in vitro. *J. Assoc. Res. Otolaryngol.* **11**, 203-222.
Shi, F., Kempfle, J. S. and Edge, A. S. B. (2012). Wnt-responsive Lgr5-expressing stem cells are hair cell progenitors in the cochlea. *J. Neurosci.* **32**, 9639-9648.
Shi, F., Hu, L. and Edge, A. S. B. (2013). Generation of hair cells in neonatal mice by β-catenin overexpression in Lgr5-positive cochlear progenitors. *Proc. Natl. Acad. Sci. USA* **110**, 13851-13856.
Srinivasan, R. S., Dillard, M. E., Lagutin, O. V., Lin, F.-J., Tsai, S., Tsai, M.-J., Samokhvalov, I. M. and Oliver, G. (2007). Lineage tracing demonstrates the venous origin of the mammalian lymphatic vasculature. *Genes Dev.* **21**, 2422-2432.
Stone, J. S. and Cotanche, D. A. (2007). Hair cell regeneration in the avian auditory epithelium. *Int. J. Dev. Biol.* **51**, 633-647.
Sugawara, M., Murtie, J. C., Stanković, K. M., Liberman, M. C. and Corfas, G. (2007). Dynamic patterns of neurotrophin 3 expression in the postnatal mouse inner ear. *J. Comp. Neurol.* **501**, 30-37.
Taniguchi, M., Yamamoto, N., Nakagawa, T., Ogino, E. and Ito, J. (2012). Identification of tympanic border cells as slow-cycling cells in the cochlea. *PLoS One* **7**, e48544.
Taylor, R. R., Jagger, D. J. and Forge, A. (2012). Defining the cellular environment in the organ of corti following extensive hair cell loss: a basis for future sensory cell replacement in the cochlea. *PLoS One* **7**, e30577.
Tong, L., Strong, M. K., Kaur, T., Juiz, J. M., Oesterle, E. C., Hume, C., Warchol, M. E., Palmiter, R. D. and Rubel, E. W. (2015). Selective deletion of cochlear hair cells causes rapid age-dependent changes in spiral ganglion and cochlear nucleus neurons. *J. Neurosci.* **35**, 7878-7891.
Toyoshima, H. and Hunter, T. (1994). p27, a novel inhibitor of G1 Cyclin-Cdk protein kinase activity, is related to p21. *Cell* **78**, 67-74.
Walters, B. J., Yamashita, T. and Zuo, J. (2015). Sox2-CreER mice are useful for fate mapping of mature, but not neonatal, cochlear supporting cells in hair cell regeneration studies. *Sci. Rep.* **5**, 11621.
Walters, B. J., Coak, E., Dearman, J., Bailey, G., Yamashita, T., Kuo, B. and Zuo, J. (2017). In vivo interplay between p27Kip1, GATA3, ATOH1, and POU4F3 converts non-sensory cells to hair cells in adult mice. *Cell Rep.* **19**, 307-320.
Wang, Y., Rattner, A., Zhou, Y., Williams, J., Smallwood, P. M. and Nathans, J. (2012). Norrin/Frizzled4 signaling in retinal vascular development and blood brain barrier plasticity. *Cell* **151**, 1332-1344.
Wang, T., Chai, R., Kim, G. S., Pham, N., Jansson, L., Nguyen, D.-H., Kuo, B., May, L. a., Zuo, J., Cunningham, L. L. et al. (2015). Lgr5+ cells regenerate hair cells via proliferation and direct transdifferentiation in damaged neonatal mouse utricle. *Nat. Commun.* **6**, 6613.
Waqas, M., Guo, L., Zhang, S., Chen, Y., Zhang, X., Wang, L., Tang, M., Shi, H., Bird, P. I., Li, H. et al. (2016). Characterization of Lgr5+ progenitor cell transcriptomes in the apical and basal turns of the mouse cochlea. *Oncotarget* **7**, 41123-41141.
Warchol, M. E. and Corwin, J. T. (1996). Regenerative proliferation in organ cultures of the avian cochlea: identification of the initial progenitors and determination of the latency of the proliferative response. *J. Neurosci.* **16**, 5466-5477.
White, P. M., Doetzlhofer, A., Lee, Y. S., Groves, A. K. and Segil, N. (2006). Mammalian cochlear supporting cells can divide and trans-differentiate into hair cells. *Nature* **441**, 984-987.
Williams, S. E., Zenner, H.-P. and Schacht, J. (1987). Three molecular steps of aminoglycoside ototoxicity demonstrated in outer hair cells. *Hear. Res.* **30**, 11-18.
Xu, J., Ueno, H., Xu, C. Y., Chen, B., Weissman, I. L. and Xu, P. X. (2017). Identification of mouse cochlear progenitors that develop hair and supporting cells in the organ of Corti. *Nat. Commun.* **8**, 15046.
Yu, Y., Weber, T., Yamashita, T., Liu, Z., Valentine, M. B., Cox, B. C. and Zuo, J. (2010). In Vivo Proliferation of Postmitotic Cochlear Supporting Cells by Acute Ablation of the Retinoblastoma Protein in Neonatal Mice. *J. Neurosci.* **30**, 5927-5936.
Zheng, J. L., Shou, J., Guillemot, F., Kageyama, R. and Gao, W. Q. (2000). Hes1 is a negative regulator of inner ear hair cell differentiation. *Development* **127**, 4551-4560.
Zuccotti, A., Kuhn, S., Johnson, S. L., Franz, C., Singer, W., Hecker, D., Geisler, H.-S., Kopschall, I., Rohbock, K., Gutsche, K. et al. (2012). Lack of brain-derived neurotrophic factor hampers inner hair cell synapse physiology, but protects against noise-induced hearing loss. *J. Neurosci.* **32**, 8545-8553.

Table S1. Primary antibodies used for immunostaining and special staining procedures.

Protein	Host	Dilution	Special procedures	Vendor/catalog number
BrdU	Mouse	1:20	Conjugated primary AB	Invitrogen #B35130
Myosin VIIa	Rabbit	1:200	None	Proteus Biosciences #25-6790
p27^{Kip1}	Mouse	1:400	AUM, SE, 37°C AB incubation, & IgG1 secondary	Fisher #BDB610242
RFP	Mouse	1:200	SE, 37°C AB incubation, & IgG2a secondary	Rockland #200-301-379S
S100a1	Rabbit	1:100	37°C AB incubation	Abcam #AB868
Sox2	Goat	1:400	None	Santa Cruz #sc-17320

AB, antibody; AUM, antigen unmasking solution; SE, signal enhancer.

Table S2. Secondary antibodies used for immunostaining

Antibody	Dilution	Vendor/Catalog number
Alexa 488 donkey anti-goat	1:1000	Invitrogen #A11055
Alexa 488 donkey anti-rabbit	1:1000	Invitrogen #A21206
Alexa 546 donkey anti-rabbit	1:1000	Invitrogen #A10040
Alexa 568 goat anti-mouse IgG2a	1:1000	Invitrogen #A21134
Alexa 647 donkey anti-goat	1:1000	Invitrogen #A21447
Alexa 647 goat anti-mouse IgG1	1:1000	Invitrogen #A21240
Alexa 647 donkey anti-rabbit	1:1000	Invitrogen #A31573